Infrared Spectrum and Structure of Me₂TiCl₂ and Quantum Mechanical Calculations of Geometries and Force Fields for MeTiCl₃ and Me₂TiCl₂

G. Sean McGrady,* Anthony J. Downs, and Neil C. Bednall

Inorganic Chemistry Laboratory, University of Oxford, Oxford OX1 3QR, U.K.

Donald C. McKean*

Department of Chemistry, University of Edinburgh, Edinburgh EH9 3JJ, U.K.

Walter Thiel* and Volker Jonas

Organisch-Chemisches Institut, Universität Zürich, CH-8057 Zürich, Switzerland

Gernot Frenking

Fachbereich Chemie, Philipps-Universität Marburg, D-35032 Marburg, Germany

Wolfgang Scherer

Department of Chemistry, University of Oslo, Box 1033 Blindern, N-0315 Oslo, Norway

Received: September 26, 1996; In Final Form: December 17, 1996⊗

Infrared spectra have been studied over the range 4000−200 cm⁻¹ for (CH₃)₂TiCl₂, (CD₃)₂TiCl₂, (CH₂D)₂-TiCl₂, and (CHD₂)₂TiCl₂ in the gas and matrix phases. Some new spectral observations are also reported for CH₃TiCl₃ and CD₃TiCl₃. Equilibrium geometries and force fields are calculated for both Me₂TiCl₂ and MeTiCl₃ using both *ab initio* (MP2) and DFT approaches. Scale factors for the force fields were first determined in MeTiCl₃ and then transferred to Me₂TiCl₂ so as to provide accurate estimates and facilitate the assignment of the spectra of Me₂TiCl₂. Quantum mechanical (QM) calculations of infrared intensity proved to be vital in this process. A number of Fermi resonances involving skeletal bending modes below 200 cm⁻¹ are postulated. Combination and overtone evidence for these modes suggests that they occur close to their predicted positions in all cases except one. The infrared evidence from the C−H and C−D stretching regions indicates that the C−H bonds in each methyl group in Me₂TiCl₂ are equivalent and slightly weaker than those in MeTiCl₃. The H−C−H angle in Me₂TiCl₂ is found to be 109 ± 1°, about 1° less than in MeTiCl₃. These results are largely reproduced by the DFT calculations, whereas the *ab initio* values indicate little difference between the two compounds. The skeletal interbond angles in Me₂TiCl₂ are particularly sensitive to the type of QM calculation, but all calculations agree on a reduced C−Ti−C and an enlarged Cl−Ti−Cl angle, compared with the tetrahedral value. Problems arising in customary scaling procedures are addressed. The mode of thermal decomposition of the molecule is discussed.

Introduction

The last decade has witnessed extensive efforts to understand the structure and bonding in methyltrichlorotitanium, MeTiCl₃. Particular interest focused on the structure of the methyl group and the extent, if any, to which this might be affected by a Ti···H−C "agostic" interaction.[1−5] The earlier finding of an apparently flattened CH₃ group[1] was later contradicted by *ab initio*,[2,3] electron diffraction,[4] and infrared spectral studies.[5] In contrast, there has been a dearth of information regarding the dimethyl congener, Me₂TiCl₂, probably reflecting the greater thermal fragility, reactivity, and photosensitivity of the more highly methylated compound.[6−8]

The present infrared and theoretical study of the dimethyl compound, which parallels an electron diffraction investigation,[9] was undertaken as part of a continuing study of systems involving alkyltitanium compounds in which agostic behavior may be manifest.[10,11] We wished also to explore the use of "isolated" C−D stretching frequencies, ν^{is}CD, obtained from the vibrational spectra of molecules containing CH₂D groups,

as a supplement or possible alternative to the use of "isolated" C−H stretching frequencies as observed for CHD₂ moieties. The latter have proved a valuable source of quantitative information concerning methyl group geometry.[12−14] Isolated C−D stretching frequencies have been used for many years to identify different types of bonds in a variety of compounds,[15] but there has been as yet no careful examination of their quantitative significance. For such a study there is a need ideally to investigate both ν^{is}CH and ν^{is}CD in the same molecule.

In the course of the infrared measurements, *ab initio* studies of all the chloro(methyl)titanium compounds were published, the results including computed geometrical parameters.[16] The calculations on Me₂MCl₂ compounds were extended, when preliminary electron diffraction results became available, to consider a possible rationalization of the unusual skeletal bond angles found within the concept of Bent's rule.[17]

At an early stage in the analysis of the infrared spectra, it became evident that much of the usual information on which assignment of vibrational frequencies is normally based was missing. There were no Raman spectra available and the infrared spectra of the gaseous molecules failed to disclose

---

TABLE 1: Comparison of QM and Observed Geometries for MeTiCl₃ and Me₂TiCl₂

bond/Å, angle/deg	DFT		MP2		
	AE[b,c]	ECP[c]	AE[d]	ECP[c]	expt[a]
MeTiCl₃					
TiC	2.0478	2.0374	2.059	2.0406	2.047(6)
TiCl	2.2011	2.1964	2.183	2.1832	2.185(3)
CH	1.1015	1.1004	1.094	1.0889	1.098(6)
HCH	109.739	110.346	110.1	111.352	109.9(17)
ClTiCl	113.027	113.384	113.3	113.849	113.0(2)
Me₂TiCl₂[e]					
TiC	2.0591	2.0474		2.0413	2.058(3)
TiCl	2.2155	2.2109		2.2040	2.196(3)
CH_s	1.1020	1.1010		1.0892	1.111(4)
CH_a	1.1028	1.1012		1.0890	
H_aCH_a	109.341	110.077		111.321	110.8(10)
H_aCH_s	108.943	109.582		110.857	
H_aC-Ti	109.647	109.135		107.604	108.1(10)
H_sC-Ti	110.299	109.312		108.442	
CTiC	106.142	104.544		101.828	102.8(9)
ClTiCl	116.663	118.112		121.356	117.3(3)
Me₂−Me[f]					
ΔTiC	0.011₃	0.0100		0.0007	0.011(7)
ΔTiCl	0.014₄	0.0145		0.0208	0.011(4)
ΔCH_av	0.000₉	0.0007		0.0002	0.0014[g]

^{a} r_a geometries from refs 4 (MeTiCl₃) and 9 (Me₂TiCl₂). ^{b} Reference 9. ^{c} This work. ^{d} Reference 3. ^{e} s and a denote hydrogen atoms in and out of the plane of symmetry, respectively. ^{f} Changes from MeTiCl₃ to Me₂TiCl₂. ^{g} Value predicted from ν^{is}CH.

identifiable rotational contours from which the symmetry species of vibrational levels might be deduced, nor were there any spectra available for the region below 200 cm⁻¹. Interpretation would therefore have to be based on very precise predictions from scaled quantum mechanical (QM) force fields, the scale factors concerned to be transferred from the molecule that resembles Me₂TiCl₂ most closely, namely, MeTiCl₃, whose vibrational spectrum has been well, if not completely, characterized.[5] This involved us both in a re-examination of the vibrational spectra of MeTiCl₃ and also in an exhaustive study of its force field by a variety of QM methods, including both *ab initio* and DFT approaches, which were each in turn then applied to Me₂TiCl₂.

On one hand, we were concerned with scaling the force fields to a much higher degree of precision than is normal in order to distinguish vibrational modes that might lie close together. On the other, we were faced with the problem of choosing scale factors for use with types of motion in Me₂TiCl₂ that were not represented in MeTiCl₃, namely, the various kinds of skeletal bending mode. Previous experience in this area has shown that it is unwise to adopt a single scale factor for force constants relating to one type of coordinate, *e.g.* bending motions, even in the case of C−H or Si−H stretching,[18−21] if observed spectra are to be reproduced in detail. The result is a searching investigation of the strengths and weaknesses of customary scaling procedures and of the reliability with which scale factors may be transferred between similar molecules.

Results: Geometries of MeTiCl₃ and Me₂TiCl₂

Table 1 summarizes the bond lengths and angles computed for Me₂TiCl₂ and MeTiCl₃, along with the electron diffraction results for these molecules.[4,9]

A striking feature of the calculations is the relative constancy of the skeletal angles in the monomethyl compound compared with variations of 4−5° in the C−Ti−C and Cl−Ti−Cl angles in the dimethyl species. It is perhaps a coincidence that this sensitivity to the method chosen is found where there is great

difficulty in obtaining a chemical understanding of what is observed experimentally, namely, an unusually large Cl−Ti−Cl angle (117.3°) and a correspondingly small C−Ti−C one (102.8°).[9] The MP2/ECP calculation for Me₂TiCl₂ gives good agreement for the C−Ti−C angle but the poorest agreement for the Cl−Ti−Cl angle, and its H−C−H and Cl−Ti−Cl angles for MeTiCl₃ deviate most from those observed. The two DFT calculations both give angles in MeTiCl₃ in excellent agreement with those observed. The DFT/AE value for the Cl−Ti−Cl angle in Me₂TiCl₂ (116.7°) is the best one predicted, but its C−Ti−C angle (106.1°) is easily the worst.

Some lack of uniformity is also evident among the bond lengths. The DFT-based Ti−Cl distances tend to be larger than both MP2 and experimental ones, but the same is not true for the Ti−C values. While absolute accuracy in the QM bond lengths may not be better than ± 0.02 Å, previous experience indicates that *changes* in these lengths from one molecule to another, or within the same molecule, are likely to be much closer to changes found experimentally, *e.g.* from the ν^{is}CH values,[12] provided that the calculations are at the same level and with the same basis set. Accordingly we include in Table 1 the changes in the Ti−C, Ti−Cl, and C−H lengths between the monomethyl compound and the dimethyl one, estimated in the various ways. The agreement between experiment and the DFT results is most pleasing. However, the MP2 calculations fail to predict the lengthening of the Ti−C and C−H_av bonds that occurs and overestimate the lengthening found for the Ti−Cl bonds.

Concerning the structure of the methyl group, there is general agreement that the degree of asymmetry in the dimethyl compound with respect to C−H bond lengths is low throughout. With the switch from MeTiCl₃ to Me₂TiCl₂ there is a maximum lengthening of 0.0007 Å in the DFT results, which compares with a lengthening of 0.0014 Å predicted from the ν^{is}CH data (*vide infra*). The angular asymmetry of the methyl group is also small: the H_aCH_a and H_aCH_s angles differ by 0.3−0.5°. As is apparent from the Ti−C−H angles, the methyl group is tilted by less than 1°.

Results: Assignments and Force Fields for MeTiCl₃

Assignments. The main problem in establishing a reliable force field for MeTiCl₃ lies in locating the vibrations at wavenumbers below 200 cm⁻¹, no IR spectra in this region and no meaningful Raman spectra at any wavenumbers having been recorded up to now.[5] In the absence of direct observation, attempts were made to assign ν_5 (δ_sTiCl₃), ν_6 (τCH₃), ν_{11} (δ_{as}TiCl₃), and ν_{12} (ρTiCl₃) on the basis of combination bands at higher energy in the IR spectrum. Earlier[5] these had yielded values of 136, 159, 155, and 111 cm⁻¹, respectively. However, the scaled *ab initio* calculations of Krömer and Thiel[3] make it clear that the skeletal mode highest in energy ν_{11} (e), lying near 150 cm⁻¹, should be described by the symmetry coordinate $2\delta_1−\delta_2−\delta_3$, where δ is a C−Ti−Cl angle change. The proportion of carbon motion means that a more appropriate description for ν_{11} is δTiC. The lowest energy mode, ν_{12}, is then δ_{as}TiCl₃.[3]

Attempts were made to improve the experimental results in two ways. Both old and new spectra of the CH₃ and CD₃ species were scrutinized for further information regarding combination bands, with the results shown in Table 2. The assignment of a mode near 153 cm⁻¹ to ν_{11} is confirmed by the observation of an appreciable ¹³C shift of about 2 cm⁻¹. This is the only skeletal bending mode to involve perceptible carbon atom movement. The assignment of ν_5 to 131 cm⁻¹, 5 cm⁻¹ less than its previous value, is not very secure but is supported by the QM calculations. The combination band at

TABLE 2: Assignment of Low-Lying Modes from Combination Bands in MeTiCl$_3$ Species

mode		CH$_3$TiCl$_3$	CD$_3$TiCl$_3$
ν_{11}	δTiC	1527 = 1375 + 152	1149 = 1009 + 140
		1262^a = 1108^b + 154	
		1165(br) = 551 + 464 + 150	
		688 = 536 + 152	
ν_{12}	δ_{as}TiCl$_3$	662 = 551 + 111	631 = 521 + 110
ν_5	δ_sTiCl$_3$	606(br) = 464 + 153, 464 + 131	
ν_6	τCH$_3$	3140?? = 2981 + 159	

^{a} ^{13}C shift $\simeq$ 12 cm^{-1}. ^{b} ^{13}C shift $\simeq$ 10 cm^{-1}. 1108 cm^{-1} is a revised value based on new spectra.

3140 cm^{-1}, which earlier led to placing the methyl torsion ν_6 at 159 cm^{-1}, was not identified in the new spectra. This might have been due to the presence of impurity in the samples, but the evidence for ν_6 must now be considered very flimsy indeed. The new sample of CD$_3$TiCl$_3$ contained weak impurity bands at 1341 and 903 cm^{-1}, but the evidence for fundamental modes at 140 and 110 cm^{-1} is fairly good.

In an alternative approach, Raman spectra were obtained for CCl$_4$ and C$_6$H$_6$ solutions of both the CH$_3$ and CD$_3$ species, with the results reported in Table 3. A medium strength depolarized line at 175 cm^{-1} in the d$_0$ species shifted to a group of three such lines at 178, 169, and 160 cm^{-1} in the d$_3$ one. Such a shift can arise only in ν_{11}, but these solution values are much higher than the highest given by the unscaled QM calculations and the values deduced from the combination bands of the vapor (see Table 2). By contrast, the νTiC and νTiCl fundamentals were little changed from the gas-phase values. There was no sign of any polarized line due to ν_5 or of a depolarized one due to ν_{12}. We are bound to conclude that the MeTiCl$_3$ molecules are complexed in CCl$_4$ and C$_6$H$_6$ solution in such a way as to raise the energies of only the skeletal bending modes.

Among the gas-phase bands occurring above 300 cm^{-1}, one reassignment from ref 5 is plausible. The broad band at 380 cm^{-1} in CD$_3$TiCl$_3$ is better assigned as an overlapping pair consisting of ν_4 at about 385 cm^{-1} and ν_{10} at about 375 cm^{-1}. These new values are well fitted by the scaled quantum mechanical (SQM) calculations and also improve the prediction of several combination bands.

Force Fields. The symmetry coordinates employed were those of Krömer and Thiel.[3] They have the advantage that the symmetric deformation coordinates involve only the H−C−H or Cl−Ti−Cl angles. This enables us to avoid the κ factor in the more customary definition which involves H−C-Ti or C−Ti−Cl angles as well. Each QM calculation would have required a different value of κ. The earlier empirical force field[5] showed the compatibility of the CHD$_2$ data with those for the CH$_3$ and CD$_3$ species, and accordingly data for all three species were used in the scaling procedure. Uncertainties in the data were not less than 1%, to allow for the effects of anharmonicity. In the special case of the C−H and C−D stretching modes, which are much more affected by anharmonicity, the νCD values were ignored altogether, and only the ν^{is}CH datum in the CHD$_2$ species was given any weight. This procedure is potentially of use in identifying the extent to which the ν_{as}CH$_3$ and ν_sCH$_3$ bands have been displaced by Fermi resonances.

In scaling the QM force fields, the number of scale factors was increased until no significant improvement in the fit to the observed data was obtained. Table 4 shows the fits obtained in this way, and Table 5 shows the scale factors determined, seven such factors (ignoring the torsion) being sufficient. At an early stage, however, it was found that the MP2 calculations could not fit the ν_{as}TiCl$_3$ and ρMe frequencies simultaneously. This was traced to an erroneous interaction force constant, $F_{9,10}$, involving the two coordinates in question. The situation provides a salutary example of the inherent weakness of both QM force fields and of the program ASYM40, through which these force fields were scaled. In the two DFT force fields, $F_{9,10}$ has the value −0.0516 and −0.0532 aJ Å^{-1} rad^{-1}, respectively, and reproduction of the ν_{as}TiCl$_3$ and ρMe frequencies is very satisfactory (Table 4). However, in the MP2 force field, as in the earlier one of Krömer and Thiel,[3] the unscaled value lies below −0.06 aJ Å^{-1} rad^{-1}. As in most force constant programs, ASYM40 can scale an off-diagonal constant only with the geometric mean of the scale factors of the corresponding diagonal constants, a condition that makes for only a trivial change of a few percent, where 30−40% is required. This small constant has a large influence due to the close proximity of the isolated motions before coupling is introduced. In the present

TABLE 3: Raman Spectra Recorded for MeTiCl$_3$ in Solution (cm^{-1})

molecule	mode	sym	description	IR (gas)^a	Raman (C$_6$H$_6$)	Raman (CCl$_4$)
CH$_3$TiCl$_3$	ν_1	A$_1$	ν_sCH$_3$	2893.5 w	2874 ms,p	2879 ms,p
	ν_2	A$_1$	δ_sCH$_3$	1108 vw	1105 ms,p	1105 ms,p
	ν_3	A$_1$	νTiC	535.7 ms	528 m,p	526 sh
	ν_4	A$_1$	ν_sTiCl$_3$	390 m	387 vs,p	388 vs,p
	ν_5	A$_1$	δ_sTiCl$_3$	(131)	[n.o.]^b	[n.o.]^b
	ν_6	A$_2$	τCH$_3$	(159)	inactive	inactive
	ν_7	E	ν_{as}CH$_3$	2981.0 w	2969 m,dp	2979 m,dp
	ν_8	E	δ_{as}CH$_3$	1374.5 m	1364 w,dp	1365 w,dp
	ν_9	E	ν_{as}TiCl$_3$	550.5 vs	538 br,sh	538 m
	ν_{10}	E	ρCH$_3$	463.7 vs	458 w	obscured
	ν_{11}	E	δTiC	(153)	175 m,dp	170 m,dp
	ν_{12}	E	δ_{as}TiCl$_3$	(111)	[n.o.]^b	[n.o.]^b
CD$_3$TiCl$_3$	ν_1	A$_1$	ν_sCD$_3$	2099.7 w	2087 s,p	2089 s,p
	ν_2	A$_1$	δ_sCD$_3$	880 w	865 ms,p	865 ms,p
	ν_3	A$_1$	νTiC	496.5 s	488 ms,p	487 ms,p
	ν_4	A$_1$	ν_sTiCl$_3$	385 ms^c	387 vs,p	387 vs,p
	ν_5	A$_1$	δ_sTiCl$_3$	[n.o.]^b	[n.o.]^b	[n.o.]^b
	ν_6	A$_2$	τTiCD$_3$	inactive	inactive	inactive
	ν_7	E	ν_{as}CD$_3$	2238.0 w	2227 ms,dp	2229 ms,dp
	ν_8	E	δ_{as}CD$_3$	1009.3 m	998 sh	1000 w,dp
	ν_9	E	ν_{as}TiCl$_3$	520.5 vs	523 sh	520 sh
	ν_{10}	E	ρCD$_3$	375 ms^c	368 sh	370 sh
	ν_{11}	E	δTiC	(140)	179,160 m,dp	178,160 m,dp
	ν_{12}	E	δ_{as}TiCl$_3$	(110)	[n.o.]^b	[n.o.]^b

^{a} Reference 5, with alterations discussed in the text. ^{b} n.o. = not observed. ^{c} Overlapping bands (see text).

TABLE 4: Vibrational Frequency Fits (cm⁻¹) for SQM Force Fields for MeTiCl₃ Species

CH₃TiCl₃

					DFT[b]			MP2	
	observed values[a]				AE				
mode/ν	$\sigma_\nu{}^d$	$\Delta\nu^e$	$\sigma_{\Delta\nu}{}^d$	$\epsilon_\nu{}^f$	$\epsilon_{\Delta\nu}{}^f$	ECP $\epsilon_\nu{}^f$	ECP[b] $\epsilon_\nu{}^f$	AE[c] $\epsilon_\nu{}^f$
ν_1	2886.5[g]	∞	2.0	2	2.3	0.2	4.1	14.4	18.5
ν_2	1112.0[h]	11.0	10.0	2	−1.8	0.7	−1.4	4.0	−19.0
ν_3	535.7	5.4	10.5	1	−3.3	0.9	−3.3	−6.1	0.7
ν_4	390.0	3.0	2.0	2	−0.4	1.1	0.4	−0.9	−6
ν_5	131.0	3			1.8	0.6*	0.2	−1.2	−4
ν_6	159.0	5			0.0	0.0*	0.0	0.0	18
ν_7	2981.0	∞	8.3	3	−1.0	−2.4	−1.7	−5.6	−9
ν_8	1374.5	13.7	3.5	0.5	−6.6	0.3	−4.7	−7.4	7
ν_9	550.5	5.5	1.0	1	−2.3	−1.2	−3.5	0.2	−5
ν_{10}	463.7	4.6	0.5	0.5	0.4	−0.6	−0.3	−0.6	2
ν_{11}	153.0	3			−0.2	2.4*	−0.1	−0.8	2
ν_{12}	111.0	3			−0.9	0.2*	−0.3	0.4	−9

CD₃TiCl₃

					DFT[b]			MP2	
	observed values[a]				AE				
mode/ν	$\sigma_\nu{}^d$	$\Delta\nu^e$	$\sigma_{\Delta\nu}{}^d$	$\epsilon_\nu{}^f$	$\epsilon_{\Delta\nu}{}^f$	ECP $\epsilon_\nu{}^f$	ECP[b] $\epsilon_\nu{}^f$	AE[c] $\epsilon_\nu{}^f$
ν_1	2099.7	∞	5.0	4	35.9	1.2	39.1	48.5	17
ν_2	880.0	8.8	13.0	5	−0.2	1.5	−0.6	−5.2	−17
ν_3	496.5	5	4.0	3	4.3	1.8	4.6	6.4	5
ν_4	385.0	5			−2.3	1.1*	−1.7	−3.1	1
ν_5					127.4*	0.5*	128.9*	130.3*	133*
ν_6					112.9*	0.0*	112.8*	112.9*	100*
ν_7	2238.0	∞			31.3	15.0*	30.4	26.7	−8
ν_8	1009.3	10.0	4.0	3	6.3	0.3	7.2	6.6	6
ν_9	520.7	5.2	0.0	1	2.6	0.6*	2.4	4.4	2
ν_{10}	375.0	5			−0.2	2.9*	−1.0	−1.6	12
ν_{11}	140.0	2			0.4	1.3*	0.3	0.4	2
ν_{12}	110.0	2			−0.9	0.2*	−0.2	0.3	−9

CHD₂TiCl₃

		observed values[a]		DFT[b]		MP2
	mode	ν	$\sigma_\nu{}^d$	AE $\epsilon_\nu{}^f$	ECP $\epsilon_\nu{}^f$	ECP[b] $\epsilon_\nu{}^f$
A′	ν_1	2952.3	1.0	0.0	0.0	0.0
	ν_2	2165.0	∞	56.4	58.4	64.2
	ν_3	1080.0	10.8	1.5	4.3	1.5
	ν_4	935.0	9.4	1.0	0.3	−0.1
	ν_5	540.0	5.4	−2.7	−3.5	−2.3
	ν_6	510.0	5.1	2.3	2.3	3.1
	ν_7	422.0	4.2	1.7	1.0	1.6
	ν_8			386.8*	386.4*	387.7*
	ν_9			144.4*	144.5*	144.7*
	ν_{10}			127.9*	129.4*	130.8*
	ν_{11}			111.3*	110.6*	110.0*
A″	ν_{12}	2231.0	∞	24.2	23.4	19.7
	ν_{13}	1230.1	12.3	−4.2	−3.7	−3.8
	ν_{14}			518.2*	518.4*	516.5*
	ν_{15}			376.6*	377.3*	378.0*
	ν_{16}			145.1*	145.1*	145.2*
	ν_{17}			122.6*	122.6*	122.5*
	ν_{18}			111.0*	110.3*	109.8*

[a] Data from ref 5, with alterations as described in text. [b] This work. [c] Data from ref 3. [d] Uncertainty in datum observed. [e] Frequency shift ¹²C−¹³C. [f] $\epsilon_\nu = \nu_{obs} − \nu_{calc}$, except for values indicated by an asterisk, which are ν_{calc}. Similarly for $\epsilon_{\Delta\nu}$. [g] Fermi resonance correction applied. [h] Older value, quoted in ref 5.

case, a rough manual manipulation of $F_{9,10}$ suggested that a value of about −0.04 aJ Å⁻¹ rad⁻¹ is appropriate, and this has been adopted as a constraint in the MP2 force field (before scaling).

Looking closely at the variations in the scale factors in Table 5 reveals some trends that are as expected and others less so. Thus the DFT factors are generally closer to unity than the MP2 ones, although the νTiCl and skeletal bending ones are wider of the mark in DFT than in MP2.

All treatments require slightly differing factors for the asymmetric and symmetric methyl deformation constants, and this appears to be a common phenomenon.[18−21] It is clearly undesirable to assume that the $\delta_{as}CH_3$ and ρCH_3 factors can be constrained to be identical, to judge by all except the DFT/effective core potential (ECP) force field. The same is true for the νTiC and νTiCl factors. What was of concern to us throughout, with our need for accurate prediction of the unobserved skeletal bending region of Me₂TiCl₂, was the possibility that we would need differing factors for the different kinds of bending motion. The $\delta_{as}TiCl_3$ and $\delta_s TiCl_3$ data were quite well fitted by a common scale factor in all cases, but a different one

TABLE 5: Scale Factors s_{ii} for MeTiCl₃ and Me₂TiCl₂

MeTiCl₃

symmetry coordinate		DFT		MP2[a]
i	type	AE	ECP	ECP[a]
1, 7	νCH[b]	0.9573(4)	0.9601(4)	0.8824(4)
2	δ_sCH₃	0.9647(72)	1.0152(75)	0.9712(87)
8	δ_{as}CH₃	1.0071(60) ⎫	1.0306(52)	⎰ 0.9449(67)
10	ρCH₃	0.9798(104) ⎭		⎱ 1.1711(144)
3	νTiC	1.0042(84)	0.9625(79) ⎫	0.9318(55)
4, 9	νTiCl	1.0796(77)	1.0566(70) ⎭	
5	δ_sTiCl₃ ⎫		1.0551(160)	0.9591(171)
11	δ_{as}TiCl₃ ⎬	1.0860(109) ⎫		
12	δTiC ⎭	⎭	1.0189(155)	1.0155(182)
6	τCH₃[c]	(1.3778)	(1.0917)	(0.8426)

Me₂TiCl₂[d]

symmetry coordinate		DFT		MP2
i	type	AE	ECP	ECP
1, 2, 10, 11, 15, 16	νCH	0.9513(7)	0.9549(4)	0.8733(3)
5, 11, 18, 24	δ_{as}CH₃	0.9892(89)	1.0175(47)	0.9295(41)
6, 19	δ_sCH₃	0.9588(145)	1.0194(80)	0.9905(73)

[a] $F_{9,10}$ constrained = −0.04 aJ Å⁻¹ rad⁻¹ (before scaling). [b] Refined to ν^{is}CH = 2952.3 cm⁻¹ only. [c] Reproducing an assumed torsional frequency of 159 cm⁻¹. [d] Other scale factors were transferred from MeTiCl₃. Where the δTiC and δTiCl₃ factors differed, the latter was used only for the δ_sTiCl₂ coordinate S₉, the former for the δ_sTiC₂, τTiC₂, ρTiC₂, and wTiC₂ coordinates S₈, S₁₄, S₂₁, and S₂₇.

TABLE 6: SQM Force Fields for MeTiCl₃[a]

		DFT/AE	DFT/ECP	MP2/ECP		DFT/AE	DFT/ECP	MP2/ECP
A₁	$F_{1,1}$	4.8305	4.8325	4.8075	$F_{1,5}$	0.0401	0.0441	0.0358
	$F_{2,2}$	0.7533	0.7886	0.8188	$F_{2,3}$	−0.1276	−0.1338	−0.0967
	$F_{3,3}$	1.9584	1.9615	2.0123	$F_{2,4}$	−0.0654	−0.0703	−0.0581
	$F_{4,4}$	2.7818	2.7820	2.8285	$F_{2,5}$	−0.0486	−0.0493	−0.0519
	$F_{5,5}$	1.0119	1.0719	1.1357	$F_{3,4}$	0.1940	0.1944	0.1911
	$F_{1,2}$	0.1888	0.2040	0.2016	$F_{3,5}$	−0.0197	−0.0282	−0.0520
	$F_{1,3}$	0.0848	0.0845	0.0674	$F_{4,5}$	−0.0559	−0.0609	−0.0340
	$F_{1,4}$	−0.0154	−0.0173	−0.0298				
E	$F_{7,7}$	4.7936	4.7939	4.8021	$F_{8,9}$	0.0001	−0.0011	0.0000
	$F_{8,8}$	0.4951	0.4874	0.4644	$F_{8,10}$	0.0258	0.0276	0.0473
	$F_{9,9}$	2.4058	2.4073	2.3638	$F_{8,11}$	−0.0070	−0.0078	−0.0079
	$F_{10,10}$	0.1828	0.1839	0.1830	$F_{8,12}$	0.0041	0.0045	0.0047
	$F_{11,11}$	0.3578	0.3521	0.3390	$F_{9,10}$	−0.0516	−0.0532	−0.0418[b]
	$F_{12,12}$	0.4535	0.4463	0.4696	$F_{9,11}$	0.0608	0.0590	0.0712
	$F_{7,8}$	−0.1379	−0.1408	−0.1317	$F_{9,12}$	−0.0470	−0.0397	−0.0604
	$F_{7,9}$	−0.0080	−0.0053	−0.0058	$F_{10,11}$	0.0101	0.0125	0.0127
	$F_{7,10}$	0.1199	0.1233	0.1428	$F_{10,12}$	0.0379	0.0390	0.0526
	$F_{7,11}$	−0.0200	−0.0201	−0.0200	$F_{11,12}$	−0.0102	−0.0127	−0.0065
	$F_{7,12}$	0.0487	0.0504	0.0508				

[a] Units: aJ Å⁻²; aJ Å⁻¹ rad⁻¹; aJ rad⁻². [b] See text for constraint.

was needed for the δTiC motion in the two ECP calculations. The problem in transferring these to Me₂TiCl₂ was to decide which of the two factors was appropriate for the five different types of skeletal bend in the latter. In any event, it was decided to use the δ_sTiCl₃ one only for the δ_sTiCl₂ coordinate in Me₂-TiCl₂ and the δTiC factor for all four of the δ_sTiC₂, wTiC₂, τTiC₂, and ρTiC₂ skeletal motions. The uncertainty that arises from this assumption is fortunately absent with the DFT/AE (AE = all-electron) force field, where one scale factor fits all three of the MeTiCl₃ bending modes.

Elsewhere in Table 5 we can trace features related to the variations in equilibrium geometry recorded in Table 1. Thus the 8% difference in the νTiC and νTiCl factors for the DFT/AE force field may be related to the overestimate of ρTiCl but good reproduction of ρTiC when this approach is made. A final comment here concerns the scale factors quoted for the methyl torsion. These are based on an exact reproduction of an almost arbitrary torsional frequency of 159 cm⁻¹, and we can only be surprised by the very large range of torsional frequencies that each unscaled calculation yields. The QM calculations are of

little use, then, in giving us any idea of what torsional frequency to expect.

Harmonic Local Mode Calculations for MeTiCl₃. For the interpretation of the C−H stretching region of Me₂TiCl₂ it is important to know the size of the C−H stretch/C−H stretch valence interaction force constant, f'_α, and a transfer of this parameter from MeTiCl₃ proves to be essential. The constant will have slightly different values in a particular molecule depending on whether it is obtained from a complete force field or from a harmonic local mode (HLM) one which ignores all vibrations other than the C−H or C−D stretching motions. Table 7 shows the values of this parameter in MeTiCl₃ obtained from the complete SQM calculations, *e.g.* from the symmetry force constants of Table 6, and also from all six of the ν_{as}CH₃ and ν_sCH₃ frequencies yielded by the complete SQM force field, on the assumption that these are given simply by the product of the diagonal F and G elements, as implied in the HLM approach. The experimental value of f'_α in the HLM approximation was derived from the observed ν_{as}CH₃ and ν^{is}CH data, plus the best experimental angle.[4] The preferred DFT
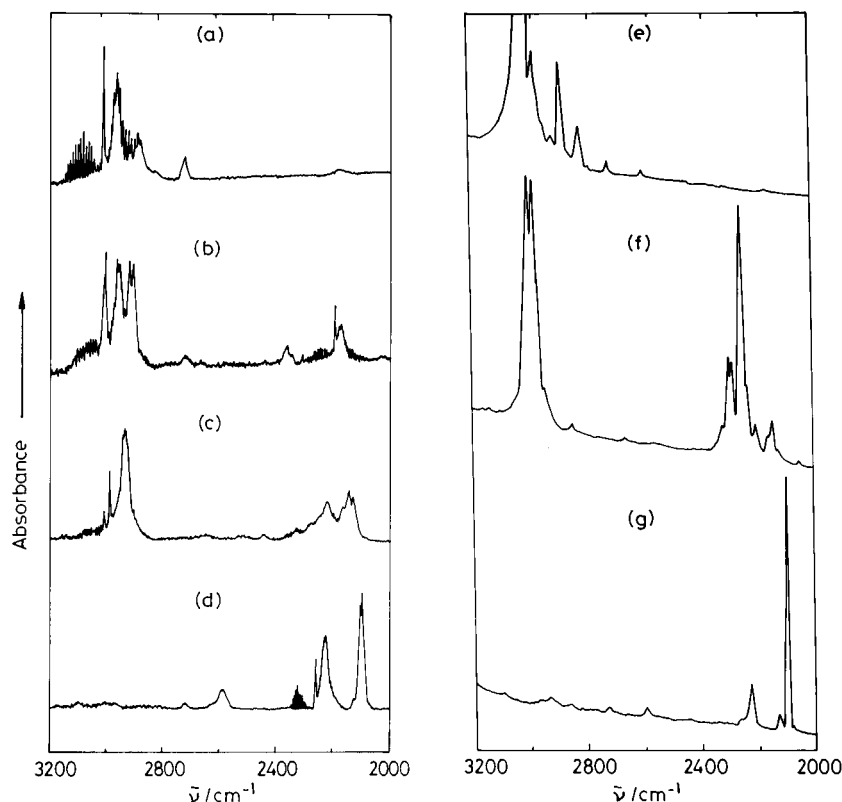
Figure 1. Absorbance IR spectra recorded for isotopomers of Me_2TiCl_2 in the region $3200-2000$ cm^{-1}. (a and e) $(CH_3)_2TiCl_2$; (b) $(CH_2D)_2TiCl_2$; (c and f) $(CHD_2)_2TiCl_2$; and (d and g) $(CD_3)_2TiCl_2$. Spectra a$-$d were measured for samples in the gas phase at ambient temperature, and e$-$g for samples isolated in an Ar matrix at 14 K.

TABLE 7: CH Stretch/CH Stretch Interaction Constants f'_α and Fit to $\nu_{as}CH_3$ and ν_sCH_3 Frequencies in CH_3TiCl_3

	DFT[a]		MP2		
	AE	ECP	AE[c]	ECP[a]	expt[b]
$f'_\alpha(full)^d$	0.0129	0.0128	-0.0127	0.0018	0.022
$\epsilon_\nu(\nu_{as}CH_3)^e$	-1.0	-1.7	-9	-5.6	0.0
$\epsilon_\nu(\nu_sCH_3)^e$	2.3	4.1	18.5	14.4	2.2
$f'_\alpha(HLM)^f$	0.0205	0.0216	-0.0037	0.0122	0.025
HCH angle	109.739	110.346	110.1	111.352	110.23[b]

[a] This work. [b] Reference 5, average of the CH_3TiCl_3 and CD_3TiCl_3 values. [c] Reference 3. [d] Value of stretch/stretch interaction constant from the complete force field treatment; units aJ Å^{-2}. [e] $\nu_{obs} - \nu_{calc}$, based on $\nu_{as}CH_3 = 2981$ cm^{-1}, $\nu_sCH_3 = 2886.5$ cm^{-1}.[5] [f] Value of stretch/ stretch interaction constant from harmonic local mode treatments of the SQM calculated frequencies (scaled on $\nu^{is}CH$) or (column 5) the experimental $\nu_{as}CH_3$ and $\nu^{is}CH$ values.

treatments agree in finding f'_α (full) to be about 0.013 aJ Å^{-2}, with the HLM value about 0.008 larger at 0.021 aJ Å^{-2}. The MP2 treatments yield consistently smaller values.

Table 7 also includes the differences between observed and calculated $\nu_{as}CH_3$ and ν_sCH_3 frequencies in each approach. Bearing in mind that a somewhat uncertain Fermi resonance correction of 7 cm^{-1} was applied in ref 5 to the observed ν_s-CH_3 datum, the DFT/AE result is very satisfactory, suggesting that this correction should actually be about 9 cm^{-1}. Perhaps the oddest feature of this table, though, is the poor reproduction of the observed data by the MP2/AE force field.[3]

Results and Discussion: Me_2TiCl_2

Selected infrared spectra are illustrated in Figures 1 and 2, while Tables 8$-$11 give the infrared results collected for the four isotopomers studied, namely d_0, d_6, d_2, and d_4, respectively. Table 12 lists the symmetry coordinates on the basis of which normal coordinates are to be described (see also Figure 3). The 27 vibrations are divided between the four symmetry species

as follows: $9A_1$, $5A_2$, $7B_1$, and $6B_2$. The B_1 and B_2 species contain the $\nu_{as}TiC_2$ and $\nu_{as}TiCl_2$ modes, respectively. Tables 13$-$16 give the frequencies and infrared intensities predicted for the d_0 and d_6 isotopomers. The intensities are calculated using the normal coordinates for the unscaled force fields. Frequency predictions for the d_2 and d_4 species are confined to the averages (weighted according to abundance) of those calculated for the four conformers present in each case on the basis of the DFT/ECP force field only, and these are included in Tables 10 and 11. In each case error limits in parentheses show the extreme range of frequency covered by the four conformers. Since there are four ways of obtaining a $CH_sD_2CH_aD_2$ conformer, compared with two for each of the $CH_aD_2CH_aD_2$ ones and only one for the solitary $CH_sD_2CH_sD_2$ conformer, the averages lie close to the frequencies of H_sH_a species.[22]

The bases of the SQM predictions are scale factors transferred from those for $MeTiCl_3$ and supplemented by ones for the νCH, $\delta_{as}CH_3$, and δ_sCH_3 coordinates which were obtained by refinement to the observed $\nu^{is}CH$, $\delta_{as}CH_3$, and δ_sCH_3 band frequencies.[22] These are all summarized in Table 4.

Discussion of the assignments falls naturally into three regions, namely, $3000-800$, $600-300$, and <150 cm^{-1}. The first of these includes the internal modes of the methyl groups, excluding rocking, the second includes the skeletal stretching and the methyl rocking fundamentals, and the third involves the skeletal bending and methyl torsion modes. With one possible and useless exception, no recognizable rotational contours could be discerned in any of the spectra of gaseous samples.

Region 3000$-$800 cm^{-1}. Parts c and b of Figure 1 show a well-defined single band at 2938 and 2176 cm^{-1} for the gaseous d_4 and d_2 species, respectively; this is attributable to the stretching of a single type of C$-$H or C$-$D bond. While the bandwidths observed could admit a variation of several cm^{-1} in such frequencies, they will also reflect small couplings
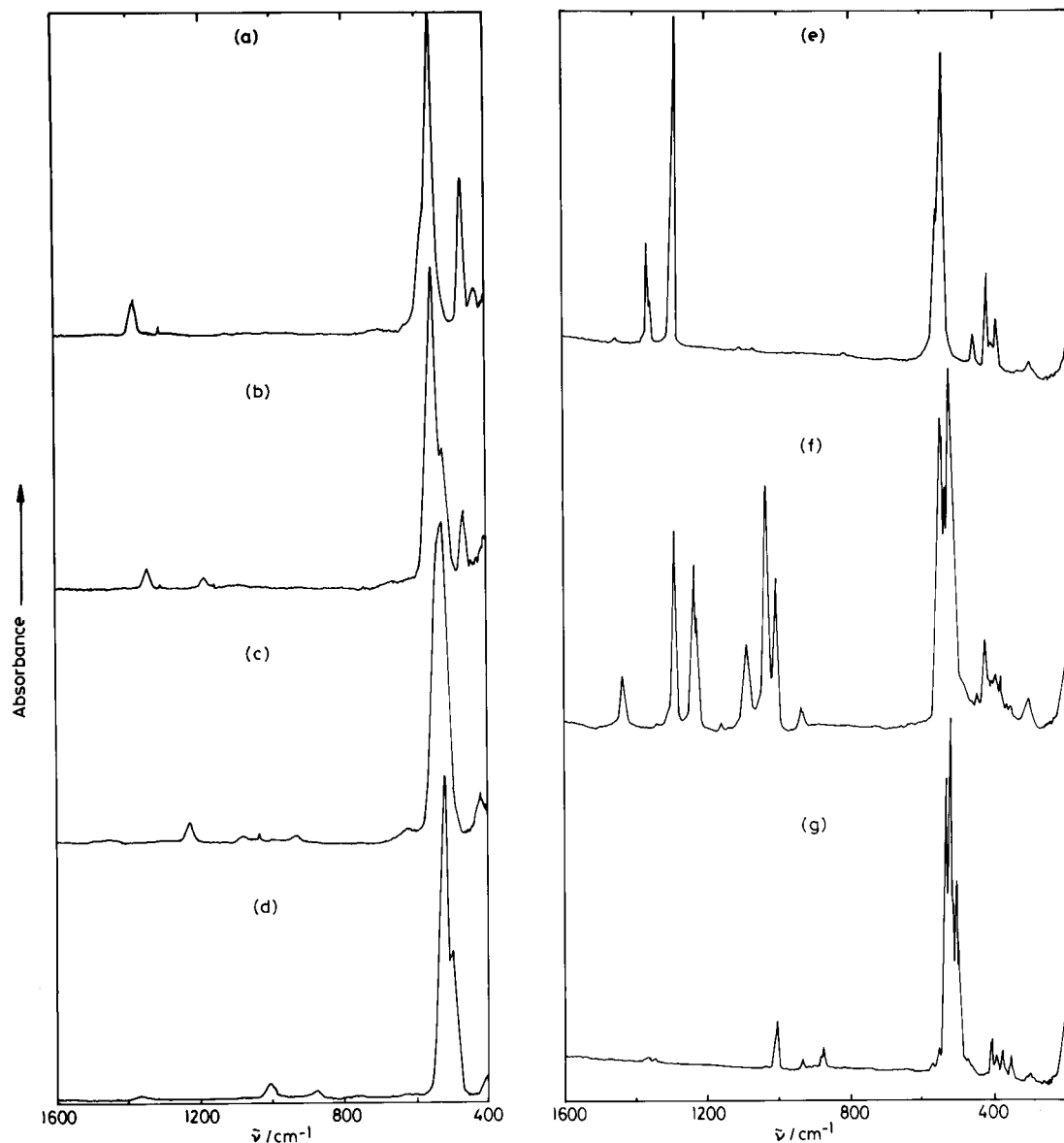
Infrared Spectrum and Structure of Me$_2$TiCl$_2$

J. Phys. Chem. A, Vol. 101, No. 10, 1997 **1957**

Figure 2. Absorbance IR spectra recorded for isotopomers of Me$_2$TiCl$_2$ in the region 1600−400 cm^{-1} (a−d) or 1600−200 cm^{-1} (e−g). (a and e) (CH$_3$)$_2$TiCl$_2$; (b) (CH$_2$D)$_2$TiCl$_2$; (c and f) (CHD$_2$)$_2$TiCl$_2$; and (d and g) (CD$_3$)$_2$TiCl$_2$. Spectra a−d were measured for samples in the gas phase at ambient temperature, and e−g for samples isolated in an Ar matrix at 14 K.

between the C−H or C−D bonds in the (CHD$_2$)$_2$ or (CH$_2$D)$_2$ conformers present. The largest coupling in the (CH$_2$D)$_2$ family is calculated to be 2.6 cm^{-1} for two C−H$_a$ bonds on the same side of the molecule; for two C−H$_s$ bonds the same calculation gives 1.0 cm^{-1}. The DFT/AE calculation predicts an 8.9 cm^{-1} difference between the ν^{is} values for the C−H$_s$ and C−H$_a$ bonds, reflecting the 0.0008 Å difference in their computed lengths (Table 1), but it is doubtful if this could be accommodated in the bandwidth observed. Within the reasonable error inherent in both approaches, the C−H bonds may be considered to be identical.

Matrix spectra were not available for the d$_2$ species. For the d$_4$ isotopomer, the region is partly obscured by strong CH$_2$D$_2$ and CHD$_3$ impurity bands (see Figure 1f), but only a single, sharp shoulder at 2942 cm^{-1} could be seen. This evidence points to the presence of only a single type of C−H bond in the matrix, as in the gas phase.

Differing C−H bond strengths would of course be reflected in splittings of the ν_{as}CH$_3$ and ν_{as}CD$_3$ bands. The latter is seen in Figure 1d at 2225 cm^{-1}, well clear of methane impurity bands, and is certainly a singlet. Its width is slightly greater than that of the ν_sCD$_3$ band at 2099 cm^{-1}, but this is normal for such

modes. The corresponding CH$_3$ bands in the d$_0$ species in Figure 1a are unfortunately overlapped by lines of the ν_3 CH$_4$ impurity band, although both appear to be broad. The same is true of the ν_{as}CH$_2$ band in the d$_2$ species in Figure 1b. Absorptions in this case at 2924 and 2911 cm^{-1} may both be associated with ν_sCH$_2$, the band being centered at 2919 cm^{-1}, where there is a weak Q branch. The P−R spacing for an A-type band in Me$_2$TiCl$_2$ is calculated to be about 12 cm^{-1}, so that interpretation of the observed features as being due to such a band is plausible. This would then constitute the only example of a rotational contour in any of the spectra. However, there will be a wide range of dipole derivative directions in the various conformers, as well as some variation in frequency, and other interpretations of the features near 2920 cm^{-1} seem more likely.

Since ν_sCH$_3$ levels are normally in Fermi resonance with $2\delta_{as}$CH$_3$ and $2\delta_s$CH$_3$ levels, it is important to identify these overtone bands. In (CH$_3$)$_2$TiCl$_2$ the overtone band due to $2\delta_{as}$CH$_3$ at 2728.5 cm^{-1} is quite strong, in contrast to the situation in CH$_3$TiCl$_3$, suggesting a higher degree of Fermi resonance in the dimethyl compound. The position of δ_{as}CH$_3$ near 1375 cm^{-1} is identical with that in CH$_3$TiCl$_3$ (1374.5 cm^{-1}). There is no sign of a band due to $2\delta_s$CH$_3$. The corresponding

1958 *J. Phys. Chem. A, Vol. 101, No. 10, 1997*

McGrady et al.

TABLE 8: Infrared Bands (cm^{-1}) for (CH$_3$)$_2$TiCl$_2$[a]

N$_2$ matrix	Ar matrix	gas phase	assignment[b]
3526 vw	3522 vw	3518 vw	548 + 2978 = 3526*(A$_1$,B$_1$,B$_2$)
3440 vw	3435 vw	3430 vw	548 + 2888 = 3436*(A$_1$,B$_1$)
3013 vs	3014 vs	3017 w	CH$_4$
2978 w	2978 w	~2967 w	ν_{as}CH$_3$, ν_1 (a$_1$), ν_{15} (b$_1$), ν_{22} (b$_2$)
2968 w	2925 sh		
	2914 vw		CH$_4$
2882 m	2888 mw	2893.5 mw	ν_sCH$_3$, ν_2 (a$_1$), ν_{16} (b$_1$)
2821 w	2820 w	2832 vw	CH$_4$
2717 vw	2719 vw	2728.5 w	2 × 1375 = 2750(A$_1$,B$_1$), FR
2601 vw	2601 vw		CH$_4$
2330 vw			CO$_2$
		2182 vw	2 × 1086(A$_1$)?
		1929 vw	552 + 1375 = 1927(A$_1$,B$_1$,B$_2$)
1842 vw,br	1840 vw	1840 vw	1375 + 463 = 1838(A$_1$,B$_1$,B$_2$)
1818 vw,br	1824 vw		1371 + 451? = 1822*(A$_1$,B$_1$,B$_2$)
	1807 vw		1371 + 426 = 1797*(A$_1$,B$_1$,B$_2$)
1786 vw	1786 vw		1371 + 424 = 1795*(A$_1$,B$_1$,B$_2$)
1676 vw	1672 vw	1672 vw	552 + 1119 = 1671(A$_1$,B$_1$)
1652 vw	1652 vw	1650 vw	1375 + 2 × 138 = 1651(A$_1$,B$_1$,B$_2$)
1620 vw	1618 vw		1079 + 548 = 1627*(B$_1$), FR
1600 w			H$_2$O
1569 vw?	1569 vw?		1117 + 461 = 1580*; 1079 + 483? = 1562*(B$_1$,B$_1$)
1531 vw			1119 + 424 = 1543*(B$_2$)?
	1509 vw		1117 + 398 = 1515*(A$_1$,B$_1$)
1475 sh	1492 sh		
1467 vw	1466 vw	1473 vw	1371 + 103 = 1474*(A$_1$,B$_1$,B$_2$)
1447 vw	1453 vw		δ_{as}CH$_3$ + τCH$_3$?
	1439 vw		δ_{as}CH$_3$ + τCH$_3$?
1374.5 s	1375.5 s	1379.0 ms	δ_{as}CH$_3$, ν_{24} (b$_2$)
1368.0 ms	1369.0 ms	1374.5 ms	δ_{as}CH$_3$, ν_3 (a$_1$)
		1371.5 sh	δ_{as}CH$_3$, ν_{17} (b$_1$)
1305 s	1305 s	1305 w	CH$_4$
		1273 vw	1119 + 152 = 1271(A$_1$,B$_1$)
1119 w,br	1117 w	1119 vw	δ_sCH$_3$, ν_4 (a$_1$), ν_{18} (b$_1$)
1079 w	1079 w	1086 vw	552 + 552 = 1104(B$_1$), FR
		1056 vw	576 + 483? = 1059(B$_2$)
		1008 vw	576 + 429 = 1005(A$_1$)
	992 vw		570 + 426 = 996*(A$_1$)
	954 vw	950 vw	552 + 395 = 947(B$_2$)
	914 vw		2 × 461 = 992*(A$_1$), FR
	892 vw		461 + 426 = 887*(A$_1$), FR
		852 vw	463 + 395 = 858(B$_2$); 2 × 429 = 858(A$_1$)
826 vw	823 vw ⎫		⎧ 426 + 398 = 824*(B$_2$)
	816 sh ⎭		⎩ 548 + 2 × 132,138 = 812, 824*(A$_1$)?
751 vw,br	745 vw,br		548 + 2 × 103 = 754*(A$_1$)?
698 vw	696 vw	695 vw,br	548 + 152 = 700*(A$_1$)
	570.0 s	575.5 s,sh	ν_{as}TiCl$_2$, ν_{24} (b$_2$)
557.0 vs	557.5 vs	551.5 vs	ν_{as}TiC$_2$, ν_{19} (b$_1$)
548 s,sh	548 s,sh		ν_sTiC$_2$, ν_5 (a$_1$)
		538 s,sh	395 + 152 = 547(A$_1$)
459.0 s	460.5 s	463.0 s	2 × 152 + 138 = 442*(B$_2$), FR
424.0 s	426.0 s	429.0 s	ρCH$_3$, ν_{25} (b$_2$)
407.0 mw	413.0 m		2 × 152 + 103 = 407*(A$_1$), FR
393.0 s	397.5 s	395.0 ms	ν_sTiCl$_2$, ν_7 (a$_1$)
	379 vw,sh		2 × 138 + 103 = 379*(A$_1$)
	338 vw		2 × 103 + 132 = 338*(B$_1$)?
308 mw,br	305 mw,br		3 × 103 = 309*(A$_1$)
280 xw,sh			2 × 138 = 276*(A$_1$)

[a] s strong; m medium; w weak; v very; x exceedingly; br broad; sh shoulder. [b] The asterisk identifies data based on matrix frequencies. Only the more plausible combination and overtone band assignments are given. Unobserved fundamentals are postulated as follows: A$_1$ 483, 152, 103 cm^{-1}; B$_1$ 451, 132 cm^{-1}; B$_2$ 138 cm^{-1}.

fundamental δ_sCH$_3$ is seen at 1119 cm^{-1}, some 11 cm^{-1} higher than the value for CH$_3$TiCl$_3$ (1108 cm^{-1}). It is surprising that two bands due to the a$_1$ and b$_1$ modes are not found here, as would be normal for a dimethyl compound. The δ_sCD$_3$ band in the gas is also a single feature but slightly lower in frequency than its CD$_3$TiCl$_3$ counterpart. Further consideration is given below to these observations.

The matrix ν_{as}CH$_3$ and ν_sCH$_3$ bands are less affected by neighboring absorption of methane impurity. ν_{as}CH$_3$ appears as a narrow singlet, as does ν_{as}CD$_3$. The frequencies are strange, however, in that, whereas ν^{is}CH increases slightly with the switch from the gas to the matrix and ν_{as}CH$_3$ goes up by 11 cm^{-1}, ν_sCH$_3$ goes down, and both the CD$_3$ bands hardly change their positions. This creates problems when it comes to the harmonic local mode calculations discussed below.

The matrix δ_sCD$_3$ bands exhibit the expected splittings, namely, 5.5 and 7.0 cm^{-1} in the Ar and N$_2$ matrices, respectively. The computed δ_sCD$_3$ splitting given by the DFT/ECP force field is only 2.0 cm^{-1}, but this rises to 11.3 cm^{-1} for δ_sCH$_3$, as recorded in Table 13. An even larger splitting would therefore have been expected in the spectrum of the normal methyl compound. A plausible explanation of why this is not

TABLE 9: Infrared Bands (cm^{-1}) for (CD$_3$)$_2$TiCl$_2$

N$_2$ matrix	Ar matrix	gas phase	assignment[a]
3229 vw	3226 vw	3227 vw	$2225 + 1007 = 3232(A_1,B_1,B_2)$
3221 vw	3220 vw		
3092 vw	3090 vw	3100 vw	$2225 + 878 = 3103(A_1,B_1,B_2)$
2725 vw	2725 vw	2722 vw	$2225 + 502,497 = 2727,2722(A_1,B_1,B_2)$
2596 vw	2590 vw	2589 w	$2096 + 502,497 = 2598,2593(A_1,B_1)$
	2567 vw		$2226 + 342,349 = 2568,2575*(A_1,B_1,B_2)$
2374 vw			$2102 + 2 \times 133? = 2368*(A_1,B_1)$
2332 w			CO$_2$
2258 vw	2256 vw	2257 w	CD$_4$
2246 vw	2246 vw		
2223 w	2226 w	2225 w	ν_{as}CD$_3$, ν_1 (a$_1$), ν_{15} (b$_1$), ν_{22} (b$_2$)
2123 vw	2126 vw	2122 vw	$4 \times 533(A_1)?$
		2103 w,sh	
2103.0 ms ⎱	2101.0 ms	2099 w ⎱	ν_sCD$_3$, ν_2 (a$_1$), ν_{16} (b$_1$)
2101.0 ms ⎰		2093 w ⎰	
2076 vw	2078 vw	2083 vw,sh	$4 \times 523*(A_1)?$
		2004 vw	$2 \times 1007(A_1,B_1,B_2)$
1619 vw	1625 vw	⎫	
	1609 vw	⎬	$3 \times 533,523(B_2)$
1578 vw	1593 vw	1585 w,br ⎭	
1562 vw	1560 vw		$2 \times 533 + 501 = 1567*(A_1)$
	1542 vw		$2 \times 523 + 501 = 1547*(A_1)$
	1393 vw	1390 vw,sh	$878 + 521 = 1399(B_2)?$
1375 w,sh	1376 w,sh ⎱		⎰ $1006 + 374 = 1380*(A_1,B_1,B_2)$
1368 w,br	1369 w,br ⎬	1368 w,br	$878 + 502,497 = 1380,1375(A_1,B_1)$
1362 w,sh	1363 w,sh ⎰		⎱ $1006 + 364 = 1370*(A_1,B_1,B_2)$
1345 w	1345 w		$1006 + 349 = 1355*(A_1,B_2)$
1289 vw	1287 vw		$2 \times 494 + 404 = 1392*(A_1)$
1265 vw	1268 vw	1267 vw	$1007 + 2 \times 133 = 1273(A_1,B_1,B_2)?$
1233 vw	1234 vw	1235 vw	$878 + 364 = 1242(A_1,B_1)?$
1223 vw	1223 vw	1221 vw,sh	$878 + 340,342 = 1218,1220(A_1,B_1,B_2)$
1211 vw	1209 vw	1207 vw,sh	$1007 + 2 \times 102 = 1211(A_1,B_1)$
		1089 vw	CD$_4$?, $2 \times 533 = 1066(A_1)$, FR
1032 vw	1035 vw		$2 \times 523 = 1046(A_1)$, FR
1009.0 ms	1008.0 m,sh	1007 m	δ_{as}CD$_3$, ν_3 (a$_1$), ν_{17} (b$_1$), ν_{23} (b$_2$)
1003.5 ms	1003.5 ms		
982 vw	982 vw		$2 \times 494 = 988*(A_1)$; $876 + 102 = 978*(A_1,B_1)$
931 w	932.5 w	937 vw	$531 + 403 = 934(B_2)$
	930 w,sh	923 vw	$526 + 403 = 929(B_2)$
907 w,br	907 w,br		$533 + 374 = 907*(A_1)$
895 w,br	901 w,br	896 w,sh	$501,494 + 404 = 905,898*(A_1,B_1)$
879.0 m	878.5 m ⎱	878 mw	δ_sCD$_3$, ν_4 (a$_1$), ν_{18} (b$_1$)
872.0 m	873.0 m ⎰		
863 w,sh	861 w,sh		$494 + 364 = 858*(B_1)$
	835 vw		$494 + 342 = 836*(A_1)$
		760 w,br	$403 + 364 = 767(A_1)$
749 vw,br	749 vw,br		$403 + 349 = 752*(B_2)$
632 vw,br	638 vw,br	626 w,br	$502 + 133 = 635(A_1)$; $497 + 133 = 630(A_1)$
604 vw			$499 + 105 = 604*(A_1)$
563 w	565.5 w		(CD$_3$)$_2$Zn
548 mw	550 mw		
529.0 vs	532.5 vs	531 vs,sh	$403 + 125 = 528(B_2)$, FR
519.0 vs	522.5 vs	520.5 vs	ν_{as}TiCl$_2$, ν_{24} (b$_2$), FR
	513 sh		$404 + 105 = 509*(A_1)$, FR
499.0 s	501.0 s	502.0 s	ν_sTiC$_2$, ν_5 (a$_1$)
494.0 s	494.0 s	497.0 s	ν_{as}TiC$_2$, ν_{19} (b$_1$)
468 w,sh	470 w,sh	470 w,sh	$364 + 102 = 466(A_1)$; $340 + 125 = 465(A_1)$
		446 vw	$340 + 102 = 442(B_2)$; $342 + 102 = 444(B_1)$
	415 w		$349 + \tau$CD$_3$?
400.5 ms	403.5 ms	403.0 ms	ν_sTiCl$_2$, ν_6 (a$_1$)
388.0 m	390.0 m	395 m	$3 \times 133 = 399(A_1)$, FR
373.0 m	373.5 m	375 m	ρCD$_3$, ν_{25} (b$_2$), FR
347.5 m	348.5 m	340 mw	$133 + 125 + 102 = 360(B_2)$, FR
	306 w,sh ⎱		$3 \times 102*(A_1)$
294 mw,br	294 mw,br ⎰		ternary including τCD$_3$?

[a] Asterisks indicate data based on matrix frequencies. Only the more plausible combination and overtone band assignments are given. Unobserved fundamentals assumed are A$_1$ 364, 133, 102 cm^{-1}; B$_1$ 342 cm^{-1}; B$_2$ 125 cm^{-1}.

observed is that the band due to the lower energy b$_1$ mode, ν_{18}, is in strong Fermi resonance with a combination level, producing both the observed band at 1086 cm^{-1} and a feature of higher energy coincident with bands due to the a$_1$ fundamental ν_4 at 1119 cm^{-1}. A value for the unperturbed ν_{18} of 1097 cm^{-1} would give an average δ_sCH$_3$ value of 1108 cm^{-1}, equal to

that found in CH$_3$TiCl$_3$. Such a value for ν_{18} is close to what would be expected, namely, 1094 cm^{-1}, if the actual A$_1$–B$_1$ splitting is more than twice that predicted by the DFT/ECP force field, as the matrix data for the d$_6$ species suggest. The unperturbed combination level would then need to be in the range 1108–1111 cm^{-1}.

1960 *J. Phys. Chem. A, Vol. 101, No. 10, 1997*

McGrady et al.

TABLE 10: Infrared Bands and SQM Predictions of Average Vibration Frequencies for $(CH_2D)_2TiCl_2$

ν_{obs}/cm^{-1} [a]	ν_{pred}/cm^{-1} [b] and assignment[c]
~2964 m,br,ol[d]	ν_1 2965.3(6), ν_2 2964.0(12); $\nu_{as}CH_2$
2925 ⎫	
2919 ⎬ m, A-type??	ν_3 2905.8(23), ν_4 2903.6(20); $\nu_{as}CH_2$
2911 ⎭	
2726 vw	2176 + 546
2673 vvw	2 × 1344
2367 vw	2 × 1185
2176 mw	ν_5 2168.2(18)[e], ν_6 2166.4(24)[e]; $\nu^{is}CD$
1721 vw,br	1185 + 562,548,533
1577 vw,br	1185 + 413,382
1418 vw,br	1344 + τCH_2D?
1344 m	ν_7 1351.8(17), ν_8 1346.4(34); δCH_2D (a′)
1185 m	ν_9 1179.8(35), ν_{10} 1173.8(15); δCH_2D (a″)
1099 w,br	2 × 562,548,533
1033 vw,br	ν_{11} 1040.7(16), ν_{12} 1032.4(24); δCH_2D (a′)
944 vw,br	combination or overtone
909 vw,br	combination or overtone
546 vs ⎫	ν_{13} 561.3(73), ν_{14} 546.7(58), ν_{15} 533.8(80);
518 sh ⎭	$\nu_{as}TiC_2, \nu_s TiC_2, \nu_{as}TiC_2$
461 ms	ν_{16} 470.1(119), ν_{17} 444.6(138); ρCH_2D
	ν_{18} 409.8(90), ν_{19} 378.7(34), ν_{20} 369.8(32);
	$\nu_s TiCl_2, \rho CH_2D$
	ν_{21} 152.5(13), ν_{22} 144.3(34); $wTiC_2, \delta_s TiC_2$
	ν_{23} 128.6(17), ν_{24} 125.6(13); $\tau TiC_2, \rho TiC_2$
	ν_{25} 105.8(4); $\delta_s TiCl_2$
	ν_{26} 100.5(17); $\tau CH_2D(b_2)$
	ν_{27} 73.5(11); $\tau CH_2D(a_2)$

[a] Gas phase, omitting bands due to CH_4 and CH_3D. [b] Weighted average for the four conformers present, calculated from the scaled DFT/ECP force field. The uncertainties in parentheses indicate the range covered by the four conformers. The mode numbering takes no account of any symmetry present in a particular conformer. [c] Among closely spaced modes there is frequent crossing of coordinate description between conformers. The modes near 1350, 1180, and 1040 cm^{-1} are best described by reference to the local CH_2DTi point group, C_s. [d] ol = overlapped by methane lines. [e] Computed value × 1.011 for a better comparison with observed frequencies.

The bending modes of the CH_2D and CHD_2 groups in the d_2 and d_4 species, respectively, are shown by the calculations to be highly localized within each methyl group, varying only little from one conformer to another. In the d_2 species, pairs of modes occur near 1344 (a′), 1185 (a″), and 1033 cm^{-1} (a′), all observed in the spectrum of the vapor, while similar pairs occur in the d_4 species at 1229 (a″), 1080 (a′), and 934 cm^{-1} (a′). The first and last of these are appropriately described as $\delta_s CH_2$ or $\delta_s CD_2$ modes, but for the rest reference only to the local symmetry, C_s, is preferable.

Inspection of the SQM predictions in Tables 13 and 14 shows that there is, thus far, nothing to choose between the various force fields, but this merely reflects the fact that the relevant scale factors have all been refined to the same experimental data.

Region 600−300 cm^{-1}. In this region, where the methyl rocking fundamentals couple with the various skeletal stretching vibrations, giving a series of closely spaced modes, we are entirely dependent on predictions made on the basis of the scale factors in $MeTiCl_3$. It is therefore disconcerting to find some quite large variations from one approach to the next. However, there is substantial agreement on a number of aspects. The calculations all predict that the mode highest in frequency in both the d_0 and d_6 species is ν_{24} (b_2). In the d_0 species this is a coupled $\nu_{as}TiCl_2/\rho CH_3$ mode, whereas in the d_6 species it is nearly all $\nu_{as}TiCl_2$ (Tables 13 and 14). About 20 cm^{-1} lower come the two νTiC_2 modes ν_5 (a_1) and ν_{19} (b_1). These essentially coincide in the DFT and MP2 treatments of both the d_0 and d_6 species. All three bands due to these modes are predicted to be intense in infrared absorption (Tables 15 and

16), but there is some variation of relative intensity from the MP2 calculations to the DFT ones.

Inspection of the d_0 spectra in Figure 2a,e shows a very strong band at 551 cm^{-1} (g = gas) or 557.5 cm^{-1} (m = Ar matrix) with a strong shoulder at 571 cm^{-1} (g) or 570 cm^{-1} (m). These are well explained if the lower frequency band arises from both ν_5 and ν_{19}, while the higher frequency one is due to ν_{24}. The combination band $\nu_5 + \nu_{19}$ (B_1) will then be expected at about 1102 cm^{-1} (g), close to the position needed for the supposed level in resonance with ν_{18} (b_1). ν_5, ν_{19}, and ν_{24} would then lie very close to the positions predicted by both DFT calculations. The only difficulty remaining lies in understanding why the matrix frequency of the lower energy component in the Fermi resonance (1079 cm^{-1}) falls below the gas frequency (1086 cm^{-1}) when at least one of the two fundamentals involved, ν_5 and ν_{19}, rises. The alternative of assigning one of the ν_5, ν_{19} pair to the shoulder at 538 cm^{-1} (g) is less satisfactory, since it makes for even greater difficulty in explaining the 1100 cm^{-1} region; it is also hard to account for a rise of 10 cm^{-1} with the change from gas to matrix. A combination in weak resonance with either ν_5 or ν_{19} seems a preferable explanation for the 538 cm^{-1} shoulder.

With regard to the d_6 matrix spectra, the region between 550 and 500 cm^{-1} includes four well-defined absorptions plus an additional shoulder (Figure 2g), all having their counterparts in the gas spectrum. An explanation must invoke extra combination or overtone bands. The pair 501, 494 cm^{-1} (m) or 502, 497 cm^{-1} (g) seems very close to the DFT-predicted positions for ν_5 and ν_{19}. ν_{24} is predicted to be about 30 cm^{-1} higher, with twice the intensity of either ν_5 or ν_{19}. However, not one but two very strong bands are found near 525 cm^{-1} for both the gas and matrix. If these are to be a Fermi-resonating pair involving ν_{24}, we will require a B_2 combination level at about 527 cm^{-1}.

In assigning the bands observed in the range 490−350 cm^{-1}, where four fundamentals are expected, ν_6, ν_7, ν_{20}, and ν_{25}, for both the d_0 and d_6 species, we need to be guided by the predicted infrared intensities. Of the four bands concerned, only two should exhibit appreciable intensity, namely, ν_7 and ν_{25} in the d_0 species and ν_6 and ν_{25} in the d_6 one. ν_7 (d_0) and ν_6 (d_6), which are $\nu_s TiCl_2$ modes, are both predicted by the DFT force fields to lie close to 400 cm^{-1}, and bands are found within 5 cm^{-1} of these positions. The second strong band of the d_0 species is ν_{25}, predicted at 437 (DFT/AE) or 434 cm^{-1} (DFT/ECP). In the gas as well as the matrix spectra, however, we find two prominent bands at 463, 429 cm^{-1} (g) or 461, 426 cm^{-1} (m). The band at higher frequency is significantly displaced from the predicted positions of ν_6 and ν_{20}, and again we find it preferable to postulate another Fermi resonance involving a B_2 level, in this case ν_{25}. The bands due to ν_6 and ν_{20} we consider to be near their predicted positions of about 480 and 450 cm^{-1} and too weak to be observed. Such a view is supported by slight evidence from some combination bands, as listed in Table 8. A minor resonance is also likely to be responsible for the additional weak peak at 413 cm^{-1} (m), which shifts plausibly to 415 cm^{-1} for the d_6 compound isolated in an Ar matrix.

With the d_6 species, the ρCD_3 modes ν_7, ν_{20}, and ν_{25} are expected to occur between 365 and 340 cm^{-1}, but only ν_7 and ν_{25}, both near 360 cm^{-1}, should have observable intensity in infrared absorption. Three bands of medium intensity are found in fact, although the two at higher frequency are outside the predicted range. Yet more resonances have to be envisaged. The source of their intensity may be either the bands due to ν_6 and ν_7 (wherever the latter may lie) or the band due to ν_{25}, in

TABLE 11: Infrared Bands and SQM Predictions of Average Vibration Frequencies for (CHD$_2$)$_2$TiCl$_2$

ν_{obs}/cm^{-1} [a]			ν_{pred}/cm^{-1} [b] and assignment [c]
N$_2$ matrix	Ar matrix	gas phase	
2942 sh	2942 sh	2938 w	ν^{is} CH$_s$ 2938.0(5), ν^{is}CH$_a$ 2934.8(12) [d]
		~2646 vw	2222 + 420?; 2146 + 500?
		~2525 vw	2146 + 379?
		2447 vw	2 × 1229
ol	ol	2222 w	ν_3 2218.2(6), ν_4 2217.1(3); ν_{as}CD$_2$
2147 sh	2158 sh	2164 sh ⎱	⎧ 2 × 1080, ν_5 2121.1(22),
2137 w	2141 w	2146 m ⎰	⎩ ν_6 2119.3(16); ν_sCD$_2$
		2132 w	
1588 vw,br	1585 vw,br	1594 vw	1080 + 526?
		1544 vw, br	1080 + 464?
1329 vw	1337 vw		1235 + 102?
1303 sh	1305 sh	1300 w, br	1229 + τCHD$_2$ (a$_2$, b$_2$)?
1232.5 s [e]	1234.5 s [e]	1229 m ⎱	⎧ ν_7 1230.2(17),
1224 sh	1225.5 m		⎩ ν_8 1225.3(16); δCH (a″) [f]
1155 vw	1157 vw		1077 + τCHD$_2$ (b$_2$)?
1077 sh	1077 sh	1080 w	ν_9 1075.7(38), ν_{10} 1071.0(37); δCH (a′) [f]
933 w	932 w	934 w	ν_{11} 935.2(8)
917 w	928 w		ν_{12} 931.6(9); δ_sCD$_2$ (a′) [f]
		622 sh	?
545.5 vs	547 vs	539 sh ⎱	⎧ ν_{13} 550.3(79); ν_{as}TiC$_2$
531.5 ms	531.5 s		⎨ ν_{14} 530.8(92); ν_{as}TiCl$_2$
524 vs	521 vs	526 vs ⎰	⎩ ν_{15} 516.9(74); ν_sTiC$_2$
520.5 vs			
516 sh	515 sh		
505 sh			
475 sh	490 sh		
455 sh	455 sh		
437 w	440 w		ν_{16} 427.3(252) ⎱
417 mw	419 m	418 ms	ν_{17} 403.0(231) � ν_sTiCl$_2$, ρCHD$_2$, ν_sTiC$_2$
	411 sh		
397 w	398 w		g
387 w	389 vw	383 ms	ν_{18} 385.4(139) ⎰
373 w	374 w		
356 vw	357 w		ν_{19} 362.5(94); ρCHD$_2$
346 w	347 w		ν_{20} 351.0(56); ρCHD$_2$
304 sh			
294 w,br	296 w,br		3 × 102
			ν_{21} 145.2(8), ν_{22} 139.2(15); wTiC$_2$, δ_sTiC$_2$
			ν_{23} 125.5(18), ν_{24} 121.3(19); ρTiC$_2$, τTiC$_2$
			ν_{25} 105.1(2); δ_sTiCl$_2$
			ν_{26} 90.4(15); τCHD$_2$ (b$_2$)
			ν_{27} 65.9(5); τCHD$_2$ (a$_2$)

[a] Excluding bands due to CH$_2$D$_2$ and CHD$_3$. [b] Weighted averages for the four conformers present calculated from the scaled DFT/ECP force field. The error limits indicate the range covered by all conformers. [c] See footnote c in Table 10. [d] The error limits here indicate the extent of coupling in the (CH$_s$D$_2$)$_2$ and (CH$_a$D$_2$)$_2$ species, where the H$_a$ atoms are on the same side of the skeletal plane. [e] Probably includes CH$_2$D$_2$ absorption. [f] Based on local C_s symmetry. [g] Combinations involving modes below 150 cm^{-1} also expected here.

which case the levels involved have the representation A$_1$ or B$_2$. Since the calculations put ν_{25} in the range 353−359 cm^{-1}, we suppose the pair observed at 375, 340 cm^{-1} (g) or 373, 349 cm^{-1} (m) to derive from B$_2$ levels. The band at 395 (g) or 390 cm^{-1} (m) may then be a combination of either A$_1$ or B$_1$ symmetry, leaving ν_7 unobserved or obscured by the 375 cm^{-1} band. As with the d$_0$ bands due to ν_6 and ν_{20}, we believe the fundamental bands associated with the CD$_3$ rocking modes ν_7 and ν_{20} to be unobserved in our spectra. Again, there are several combination bands at higher frequencies which suggest fundamental levels near their predicted positions of 364 and 342 cm^{-1} (Table 9).

With respect to the d$_2$ and d$_4$ species, the spectra in this region are, as might be expected, more complex. There are considerable variations in frequency and in the descriptions of the normal coordinates from one conformer to the next, and individual assignments are out of the question.

Region below 200 cm^{-1}. Despite the problem of deciding which scale factors to transfer from MeTiCl$_3$, when a particular approach requires different factors for δTiC and δTiCl$_3$ motions, there is quite good absolute agreement between the various predictions for the skeletal bending modes, as recorded in Tables

13 and 14, even if the agreement is less good on a percentage basis. As noted previously, though, the methyl torsions vary considerably.

Comparisons between Tables 14 and 15 show significant d$_0$/d$_6$ shifts in all the modes except ν_9, which is expected in the range 102−106 cm^{-1}. 3ν_9 is therefore the likely source of the broad weak band near 300 cm^{-1} displayed by all the matrix spectra. However, the H/D shift observed, 305 − 294 = 11 cm^{-1}, is substantially greater than the 4 cm^{-1} predicted for 3ν_9. The most likely explanation is a Fermi resonance in the d$_6$ species involving an A$_1$ level to higher energy. There may also be several transitions contributing to the band for either or both the d$_0$ and d$_6$ species. An alternative assignment of the 305 cm^{-1} band to 2ν_8 (2 × 152 cm^{-1}) is ruled out by the 40 cm^{-1} shift this must undergo on deuteration.

Table 8 shows that postulating two A$_1$ fundamentals at 103 and 152 cm^{-1} explains pleasingly the matrix band at 413 cm^{-1} if there is a weak resonance with the strong band due to ν_7 at 398 cm^{-1}. The B$_2$ resonance suggested above for the bands at 463 and 429 cm^{-1} (g) can then stem from a combination level 2 × 152 + 138 cm^{-1}, where 138 cm^{-1} is the supposed value of ν_{26}, down by 11 cm^{-1} from its predicted position. Two times

TABLE 12: Symmetry Coordinates S for Me_2TiCl_2

number		coordinate[a]	$1/N^2$ [b]	description	
A_1	1	$2r_1 - r_2 - r_3 + 2r_4 - r_5 - r_6$	12	$\nu_{as}CH_3$	CH_3 asym str
	2	$r_1 + r_2 + r_3 + r_4 + r_5 + r_6$	6	ν_sCH_3	CH_3 sym str
	3	$D_1 + D_2$	2	ν_sTiC_2	TiC sym str
	4	$R_1 + R_2$	2	ν_sTiCl_2	TiCl sym str
	5	$2\alpha_1 - \alpha_2 - \alpha_3 + 2\alpha_4 - \alpha_5 - \alpha_6$	12	$\delta_{as}CH_3$	CH_3 asym def
	6	$\alpha_1 + \alpha_2 + \alpha_3 + \alpha_4 + \alpha_5 + \alpha_6$	6	δ_sCH_3	CH_3 sym def
	7	$2\beta_1 - \beta_2 - \beta_3 + 2\beta4 - \beta_5 - \beta_6$	12	ρCH_3	CH_3 rock
	8	γ	1	δ_sTiC_2	TiC_2 scis
	9	δ	1	δ_sTiCl_2	$TiCl_2$ scis
A_2	10	$r_2 - r_3 - r_5 + r_6$	4	$\nu_{as}CH_3$	CH_3 asym str
	11	$\alpha_2 - \alpha_3 - \alpha_5 + \alpha_6$	4	$\delta_{as}CH_3$	CH_3 asym def
	12	$\beta_2 - \beta_3 - \beta_5 + \beta_6$	4	ρCH_3	CH_3 rock
	13	$\sum_{18}(\delta HC_iTiCl)$ $(i = 1, 2)$	18	τCH_3	CH_3 torsion
	14	$\epsilon_1 - \epsilon_2 - \epsilon_3 + \epsilon_4$	4	τTiC_2	TiC_2 twist
B_1	15	$2r_1 - r_2 - r_3 - 2r_4 + r_5 + r_6$	12	$\nu_{as}CH_3$	CH_3 asym str
	16	$r_1 + r_2 + r_3 - r_4 - r_5 - r_6$	6	ν_sCH_3	CH_3 sym str
	17	$D_1 - D_2$	2	$\nu_{as}TiC_2$	TiC_2 asym str
	18	$2\alpha_1 - \alpha_2 - \alpha_3 - 2\alpha_4 + \alpha_5 + \alpha_6$	12	$\delta_{as}CH_3$	CH_3 asym def
	19	$\alpha_1 + \alpha_2 + \alpha_3 - \alpha_4 - \alpha_5 - \alpha_6$	6	δ_sCH_3	CH_3 sym def
	20	$2\beta_1 - \beta_2 - \beta_3 - 2\beta4 + \beta_5 + \beta_6$	12	ρCH_3	CH_3 rock
	21	$\epsilon_1 + \epsilon_2 - \epsilon_3 - \epsilon_4$	4	ρTiC_2	TiC_2 twist
B_2	22	$r_2 - r_3 + r_5 - r_6$	4	$\nu_{as}CH_3$	CH_3 asym str
	23	$R_1 - R_2$	2	$\nu_{as}TiCl_2$	$TiCl_2$ asym str
	24	$\alpha_2 - \alpha_3 + \alpha_5 - \alpha_6$	4	$\delta_{as}CH_3$	CH_3 asym def
	25	$\beta_2 - \beta_3 + \beta_5 - \beta_6$	4	ρCH_3	CH_3 rock
	26	$\sum_9(\delta HC_1TiCl) - \sum_9(\delta HC_2TiCl)$	18	τCH_3	CH_3 torsion
	27	$\epsilon_1 - \epsilon_2 + \epsilon_3 - \epsilon_4$	4	$wTiC_2$	TiC_2 wag

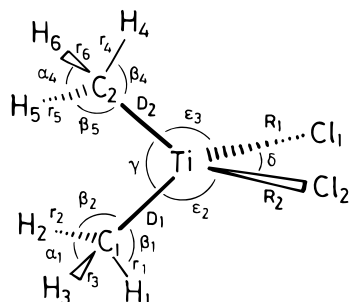[a] Internal coordinates as in Figure 3. [b] N = normalization factor.

Figure 3. Internal coordinates for Me_2TiCl_2 used in the normal coordinate analysis. ϵ_1, ϵ_2, ϵ_3, and ϵ_4 are the changes in angles between the pairs of bonds D_1R_1, D_1R_2, D_2R_1, and D_2R_2, respectively.

a fundamental at 138 cm^{-1} in combination with 103 cm^{-1} also accounts exactly for the very weak band at 379 cm^{-1}. The further very weak band at 338 cm^{-1} might involve either this same B_2 mode or else the B_1 mode predicted at 132 cm^{-1}.

If the B_2 mode ν_{26} is at 138 cm^{-1} in the d_0 species, then it should occur at about 125 cm^{-1} in the d_6 isotopomer. This is just where we need a B_2 level to account for the postulated Fermi resonance with ν_{24}, producing the bands at 531 and 521 cm^{-1} (g). We can also account for the pair at 375 and 340 cm^{-1} (g) in a similar way. The former resonance will of course occur all the way up the stack of levels $2\nu_{24}$, $3\nu_{24}$, $4\nu_{24}$, etc., with a steadily increasing resonance parameter, and the complexity of the spectra around 1600 cm^{-1} may well arise from this cause.

We have not so far invoked either the infrared-inactive A_2 mode ν_{13} or the two methyl torsions. The combinations most likely to arise from these are the torsions plus $\nu_{as}Me$ and $\delta_{as}Me$ levels. Methane absorption obscures the regions where the $\nu_{as}CH_3$, $\nu_{as}CD_3$, and $\delta_{as}CD_3$ combinations would be expected, and the only bands seen which might involve the torsions are those at 1466, 1453, and 1439 cm^{-1} displayed by the d_0 species and which could represent the levels 1373 + 93, 80, and 66 cm^{-1}, respectively. 1373 + 103 cm^{-1} is also expected in this region and may appear as the 1473 cm^{-1} band (g).

TABLE 13: SQM Predictions of Vibration Frequency (cm^{-1}) for $(CH_3)_2TiCl_2$

		DFT/ECP			DFT/AE	MP2/ECP
mode		ν	$\Delta\nu$[a]	PED[b]	ν	ν
A_1	1	2965.0	10.4	$101S_1$	2962.5	2971.1
	2	2870.5	2.4	$100S_2$	2868.7	2860.0
	3	1377.7	3.1	$98S_5$	1377.7	1377.6
	4	1119.0	9.2	$101S_6$	1119.0	1119.0
	5	553.2	9.2	$70S_3, 14S_7$	551.6	564.6
	6	475.0	6.0	$23S_3, 73S_7$	483.3	476.8
	7	398.5	1.6	$86S_4$	400.0	391.8
	8	158.9	3.4	$102S_8$	153.0	158.5
	9	106.0	0.3	$102S_9$	106.3	102.6
A_2	10	2963.2	10.6	$101S_{10}$	2956.6	2971.6
	11	1371.7	3.2	$98S_{11}$	1373.2	1368.6
	12	486.6	3.4	$94S_{12}$	488.9	491.4
	13	131.4	2.5	$12S_{12}, 100S_{14}$	134.4	138.2
	14	84.5	0.0	$10S_{12}, 106S_{13}$	69.3	91.6
B_1	15	2965.5	10.6	$101S_{15}$	2962.9	2971.6
	16	2868.7	2.4	$100S_{16}$	2867.1	2858.5
	17	1367.6	3.2	$98S_{18}$	1367.4	1369.6
	18	1107.7	9.9	$99S_{19}$	1106.7	1106.1
	19	551.9	9.7	$78S_{17}, 11S_{20}$	555.0	569.9
	20	451.0	3.5	$16S_{17}, 91S_{20}$	451.3	454.0
	21	130.0	1.3	$100S_{21}$	132.7	131.1
B_2	22	2966.3	10.6	$101S_{22}$	2959.6	2975.3
	23	1379.6	3.1	$97S_{24}$	1379.8	1377.8
	24	572.0	2.3	$35S_{23}, 44S_{25}$	572.8	589.2
	25	433.9	1.0	$60S_{23}, 55S_{25}$	437.2	426.5
	26	148.9	2.2	$97S_{27}$	149.5	149.6
	27	116.5	0.1	$101S_{26}$	103.4	134.5

[a] Frequency shift $\nu(^{12}CH_3)_2TiCl_2 - \nu(^{13}CH_3)_2TiCl_2$. [b] Diagonal terms in the potential energy distribution $\geq 10\%$.

Methyl torsions usually rise in frequency with the switch from the gas to the condensed phase, so that if the 1466 cm^{-1} band (m) does involve a torsion, then the 1473 cm^{-1} band (g) probably does not.

While the amount of H or D motion in the skeletal bending modes is small, it is enough to cause crossing over of assignment in the pairs of d_2 or d_4 bands near 145 and 130 cm^{-1} (d_2) or 140 and 126 cm^{-1} (d_4). Nevertheless, the motions δ_sTiCl_2,

TABLE 14: SQM Predictions of Vibration Frequency (cm^{-1}) for (CD$_3$)$_2$TiCl$_2$

mode		ν	$\Delta\nu^a$	PED^b	ν	ν
			DFT/ECP		DFT/AE	MP2/ECP
A$_1$	1	2216.7	14.7	102S_1	2214.5	2222.3
	2	2076.2	3.7	101S_2	2077.1	2066.0
	3	1000.4	3.7	99S_5	1000.0	999.7
	4	882.9	14.4	17S_3, 93S_6	882.1	892.5
	5	505.1	4.8	62S_3, 21S_4	503.5	509.4
	6	401.7	3.8	21S_3, 54S_4, 10S_7	404.1	399.1
	7	357.5	3.0	23S_4, 74S_7	363.7	357.7
	8	138.7	2.0	15S_9, 97S_8	133.3	137.6
	9	104.6	0.4	98S_9	105.0	101.2
A$_2$	10	2216.9	14.9	102S_{10}	2211.5	2222.4
	11	996.4	3.7	98S_{11}	997.2	993.2
	12	371.2	3.5	89S_{12}	372.7	375.6
	13	116.7	1.5	19S_{12}, 100S_{14}	119.8	121.3
	14	60.3	0.0	107S_{13}	49.4	65.9
B$_1$	15	2218.1	14.8	101S_{15}	2215.8	2224.0
	16	2052.1	3.7	101S_{16}	2075.1	2064.5
	17	993.3	3.6	98S_{18}	992.6	993.6
	18	880.9	15.1	18S_{17}, 88S_{19}	879.2	890.4
	19	497.2	5.5	74S_{17}, 11S_{19}	499.6	508.3
	20	341.2	2.7	97S_{20}	342.3	342.3
	21	123.2	0.9	98S_{21}	125.8	124.6
B$_2$	22	2218.8	14.8	102S_{22}	2189.2	2226.9
	23	1001.2	3.6	98S_{24}	1000.9	999.0
	24	532.1	1.0	68S_{23}, 12S_{25}	531.6	542.0
	25	355.4	2.4	29S_{23}, 82S_{25}	359.4	353.0
	26	134.6	1.2	12S_{25}, 96S_{27}	134.9	135.0
	27	82.8	0.0	101S_{26}	73.5	95.9

^{a} Frequency shift $\nu(^{12}CD_3)_2TiCl_2 - \nu(^{13}CD_3)_2TiCl_2$. ^{b} Diagonal terms in the potential energy distribution $\geq$ 10%.

TABLE 15: QM Predictions of Unscaled Frequencies, ω in cm^{-1}, and Infrared Intensities, A in km mol^{-1}, for the IR-Active Bands of (CH$_3$)$_2$TiCl$_2$

mode		ω_{ECP}	A_{ECP}	ω_{AE}	A_{AE}	ω_{ECP}	A_{ECP}
			DFT			MP2	
A$_1$	1	3034.7	2.0	3037.7	4.4	3180.5	0.1
	2	2937.7	0.4	2941.3	0.1	3060.6	1.5
	3	1365.6	9.1	1385.4	12.9	1424.9	6.8
	4	1109.1	5.4	1142.1	5.7	1125.6	6.7
	5	558.3	73.0	549.4	83.9	577.3	80.7
	6	471.0	1.0	485.8	0.0	453.7	8.8
	7	388.7	19.7	387.0	22.0	401.2	21.7
	8	157.4	0.0	147.2	0.0	156.7	0.0
	9	103.2	1.2	102.1	2.2	104.8	1.9
B$_1$	15	3035.2	0.6	3038.0	1.3	3180.9	0.1
	16	2935.9	3.1	2939.6	2.3	3059.1	8.8
	17	1355.6	7.1	1375.0	9.9	1416.3	5.6
	18	1098.3	8.6	1129.3	8.5	1113.2	6.8
	19	559.4	74.4	554.6	79.7	583.7	61.3
	20	446.1	0.9	455.0	2.4	424.9	0.1
	21	128.8	1.6	127.5	0.1	130.1	3.5
B$_2$	22	3036.0	6.2	3034.7	11.5	3184.9	2.5
	23	1367.5	17.5	1387.5	24.1	1424.4	16.5
	24	560.9	88.3	566.2	96.1	578.4	136.1
	25	424.6	43.9	429.1	52.4	417.3	45.2
	26	147.3	0.9	143.5	0.7	151.2	0.3
	27	111.6	0.0	88.2	0.0	143.9	0.0

TABLE 16: QM Predictions of Unscaled Frequencies, ω in cm^{-1}, and Infrared Intensities, A in km mol^{-1}, for the IR-Active Bands of (CD$_3$)$_2$TiCl$_2$

mode		ω_{ECP}	A_{ECP}	ω_{AE}	A_{AE}	ω_{ECP}	A_{ECP}
			DFT			MP2	
A$_1$	1	2244.2	0.4	2246.0	1.1	2353.5	0.0
	2	2101.8	1.1	2106.4	0.8	2187.0	2.1
	3	991.7	5.7	1005.4	8.1	1035.1	4.4
	4	877.6	15.1	898.4	14.3	901.3	18.7
	5	507.9	65.5	499.7	76.4	521.9	74.4
	6	395.8	13.0	397.1	11.8	408.5	21.1
	7	351.2	1.9	360.7	3.8	339.6	0.3
	8	137.2	0.0	128.6	0.0	135.7	0.1
	9	101.8	1.2	100.8	2.1	103.2	1.8
B$_1$	15	2245.6	0.1	2247.3	0.2	2355.2	0.0
	16	2100.2	4.2	2104.9	3.6	2185.4	7.6
	17	984.6	3.7	998.1	5.5	1028.7	3.1
	18	876.3	25.3	894.9	24.2	900.1	20.8
	19	503.3	56.1	499.7	63.7	520.5	44.7
	20	336.7	0.0	345.5	0.0	319.4	0.4
	21	122.2	1.5	120.9	2.9	123.6	3.2
B$_2$	22	2246.3	2.1	2244.8	3.9	2358.3	0.6
	23	992.5	9.8	1006.4	14.0	1034.0	9.0
	24	519.7	119.6	516.2	133.6	548.2	166.9
	25	349.1	10.5	358.4	10.9	335.8	13.5
	26	133.2	0.6	129.9	0.4	133.7	0.3
	27	79.4	0.0	62.9	0.0	104.3	0.0

symmetry force constants on which the predictions in Tables 13 and 14 are founded.

Three additional kinds of information are normally utilized to establish the origins of vibrational bands.

(i) Raman spectra would of course help to identify A$_1$ transitions through the polarization properties of the lines characterizing the molecules in the fluid phases. However, the formidable experimental difficulties experienced in attempting to measure useful Raman spectra for MeTiCl$_3$ suggest that similar experimental results may be impossible to obtain for the more reactive and thermally sensitive Me$_2$TiCl$_2$.

(ii) The second kind of information normally available is provided by the more or less well-resolved contours of the infrared bands of gaseous samples. As noted above, only one, very dubious contour was recorded in this work, namely, for the band of the d$_2$ species at 2919 cm^{-1} (Table 10). A possible reason why recognizable envelopes were so scarce in our present spectra is a proliferation of hot bands resulting from the many low-lying skeletal and torsional levels. In addition, many molecules are likely to be in states above the barrier to methyl internal rotation.

(iii) A third source of information is the ^{13}C frequency shift, which in favorable circumstances may be able to distinguish fundamentals from combination or overtone bands. Where Fermi resonance exists, conservation of ^{13}C shift during the perturbation should be maintained. Tables 13 and 14 include the shifts calculated from the DFT/ECP force field, and these should provide a useful guide to assignment when ^{13}C-labeled samples of (CH$_3$)$_2$TiCl$_2$ become available. Chlorine isotope shifts have also been calculated, but these were found to be too small to be detectable in the sort of spectra we have measured.

Harmonic Local Mode (HLM) Treatment and Structure of the Methyl Group. To extract information about the H−C−H angle in the methyl group (assumed to have C$_{3v}$ local symmetry), it was decided to utilize the interaction constant f'_α determined in the complete DFT/AE force field, with a correction of 0.008 aJ Å^{-2}.

Refining to the solitary ν^{is}CH value of 2938 cm^{-1}, the νCH and νCD frequencies are shown in Table 18 for four different H−C−H angles (107, 108, 109, and 110°) and for two values of f'_α (0.022 and 0.03 aJ Å^{-2}). Bearing in mind the breadth of

wTiC$_2$, ρTiC$_2$, and τTiC$_2$ tend to remain distinct in each conformer, without mixing.

General Force Field. It will be apparent from the preceding discussion that the tentative assignments proposed assume that the predictions based on the DFT force fields are reliable in all respects except for the B$_2$ skeletal bending fundamental ν_{26}, which we place about 11 cm^{-1} lower than its calculated value. It seemed premature to rescale either of these force fields at the present time until firmer evidence was available. We have therefore merely listed in Table 17 the scaled DFT/ECP

TABLE 17: Scaled Symmetry Force Constants for Me$_2$TiCl$_2$ from the DFT/ECP Calculation[a]

	S									
A$_1$	1	4.7463								
	2	0.0030	4.7850							
	3	−0.0063	0.0660	2.0384						
	4	0.0062	−0.0097	0.2111	2.5325					
	5	−0.1416	0.0002	0.0034	0.0003	0.4938				
	6	0.0052	0.2132	−0.1503	−0.0701	0.0002	0.7667			
	7	0.1339	−0.0017	−0.0180	0.0298	0.0276	0.0084	0.1587		
	8	0.0666	−0.0157	−0.0090	0.0329	0.0187	0.0150	0.0456	0.4891	
	9	−0.0126	0.0163	0.0129	−0.0599	−0.0094	−0.0235	0.0257	0.0887	0.3882
A$_2$	10	4.7324								
	11	−0.1450	0.4873							
	12	0.1228	0.0283	0.1621						
	13	−0.0030	−0.0021	0.0036	0.0017					
	14	−0.0304	0.0033	−0.0595	0.0009	0.3591				
B$_1$	15	4.7402								
	16	0.0080	4.7804							
	17	0.0054	0.0798	1.8336						
	18	−0.1394	0.0000	0.0028	0.4859					
	19	−0.0078	0.2102	−0.0736	−0.0001	0.7338				
	20	0.1161	−0.0028	0.0382	0.0264	−0.0143	0.1548			
	21	−0.0289	−0.0234	−0.0356	−0.0030	0.0429	−0.0207	0.3733		
B$_2$	22	4.7443								
	23	0.0066	2.2789							
	24	−0.1399	0.0034	0.4921						
	25	0.1239	0.0751	0.0302	0.1762					
	26	−0.0006	0.0011	−0.0018	0.0013	0.0029				
	27	−0.0627	−0.0967	−0.0102	−0.0437	0.0021	0.3910			

[a] Scale factors transferred from MeTiCl$_3$ except those for the νCH, δ_{as}CH$_3$ and δ_sCH$_3$ coordinates, which were refined to Me$_2$TiCl$_2$ gas-phase data. Units aJ Å^{-2}, aJ Å^{-1} rad^{-1}, and aJ rad^{-2}.

TABLE 18: Harmonic Local Mode (HLM) Calculations for Me$_2$TiCl$_2$, Fitting ν^{is}(gas) = 2938 cm^{-1}

		∠HCH							
		107°		108°		109°		110°	
group	ν_{obs}[a]	ϵ_ν^b (1)	ϵ_ν^b (2)	ϵ_ν^b (1)	ϵ_ν^b (2)	ϵ_ν^b (1)	ϵ_ν^b (2)	ϵ_ν^b (1)	ϵ_ν^b (2)
CH$_3$	2967[c]	4.8	6.9	3.2	5.3	1.6	3.7	0.1	2.2
	2893	10.9	5.6	15.0	9.8	19.2	14.0	23.4	18.1
CD$_3$	2225[c]	5.4	7.0	3.1	4.6	0.8	2.3	−1.5	0.0
	2096[d]	0.4	−3.4	6.1	2.3	11.8	8.0	17.4	13.6
CH$_2$D	2964	1.8	3.9	0.2	2.3	−1.4	0.7	−2.9	−0.8
	2919	7.5	5.1	9.4	7.0	11.2	8.8	13.0	10.7
	2176	0.3	−0.3	1.0	0.4	1.8	1.1	2.5	1.9
CHD$_2$	2938	0.0	0.0	0.0	0.0	0.0	0.0	0.0	0.0
	2222	2.4	4.0	0.1	1.6	−2.2	−0.7	−4.5	−3.0
	2146[e]	11.4	9.0	14.8	12.4	18.1	15.7	21.5	19.1
parameter									
W[f]		40.9	29.8	47.4	38.9	52.8	45.9	57.5	51.5
Δ_{anh}[g]		10.6	15.9	6.5	11.7	2.3	7.5	−1.9	3.4

[a] Gas-phase data/cm^{-1} uncorrected for Fermi resonance. [b] $\epsilon_\nu = \nu_{obs} - \nu_{calc}$. Computed νCD × 1.011 to offset anharmonicity. (1) and (2) denote results for $f'_\alpha = 0.022$ and 0.03 aJ Å^{-2}, respectively. [c] Assumed doubly degenerate. [d] Mean of two peaks. [e] Center component of three peaks. [f] Fermi resonance parameter (cm^{-1}). [g] Anharmonicity difference $2 \times \delta_{as}$CH$_3$ − $2\delta_{as}$CH$_3°$ (cm^{-1}).

the ν_{as}CH$_3$ and ν_{as}CH$_2$ bands observed, the reproduction of these is quite good at 109° for $f'_\alpha = 0.022$ aJ Å^{-2}, but the reproduction of the better defined ν_{as}CD$_3$ band is distinctly poor at 107 and 110°. The ν^{is}CD value is best reproduced with an angle of 107°, but the 2 cm^{-1} error at 109° is certainly within the accuracy of the frequency measurement and also within the likely error associated with the correction factor of 1.011, which had been applied to allow for the effects of anharmonicity.[23] There is a rather wider choice of angle with respect to the calculated positions of the symmetric stretching modes for CH$_3$, CD$_3$, and CH$_2$ moieties. At 110° the errors are 23, 17, and 13 cm^{-1}, respectively. These have an important effect on the resulting Fermi resonance corrections, as reflected in the resonance parameter W and also in the anharmonicity deficit $\Delta_{anh} = 2 \times \delta_{as}CH_3$ − $2\delta_{as}$CH$_3°$. These last quantities are shown in Table 18 for each choice of angle and f'_α. Typical values for W and Δ_{anh} for a

methyl group are around 32 and 12 cm^{-1}, respectively.[24] For MeTiCl$_3$, the 9.2 cm^{-1} shift in ν_sCH$_3$ suggested above (see Table 7) implies $W = 38.1$ cm^{-1} and $\Delta_{anh} = 12.9$ cm^{-1}.

For the dimethyl compound, calculation of Δ_{anh} involves the additional difficulty of what value to use for δ_{as}CH$_3$. Here we opt for an average of 1375 cm^{-1} based on the observed spectra together with the best predictions of all four modes as given in Table 13. The large value of W and the negative value of Δ_{anh} at 110° rule out an angle as large as this. At 109° and with $f'_\alpha = 0.022$ aJ Å^{-2}, W is still uncomfortably high and Δ_{anh} low. W is markedly reduced if f'_α is allowed to rise to 0.03 aJ Å^{-2}, but then the ν_{as}Me data are poorly fitted. While the frequency data for the δ_{as}CH$_3$ overtones are very similar for the mono- and dimethyl compounds, there does seem to be a real change in the overtone intensities relative to the ν_sCH$_3$ band, suggesting that W is higher in Me$_2$TiCl$_2$.

TABLE 19: HLM Calculations for Me$_2$TiCl$_2$, Fitting ν^{is}CH(matrix) = 2942 cm^{-1}

∠HCH =		107°		109°		111°	
f'_α/aJ Å^{-2} =		0.022	0.03	0.022	0.03	0.022	0.03
group	ν_{obs}[a]	ϵ_ν	ϵ_ν	ϵ_ν	ϵ_ν	ϵ_ν	ϵ_ν
CH$_3$	2978	11.7	13.8	8.6	10.7	5.6	7.6
	2888	2.0	−3.2	10.3	5.1	18.7	13.4
CD$_3$	2222	3.4	4.9	−1.3	0.3	−5.8	−4.3
	2101	2.6	−1.2	14.0	10.2	25.3	21.5
parameter							
W/cm^{-1}		18.3		40.4	28.9	53.0	45.7
Δ_{anh}/cm^{-1}		21.0	26.2	12.7	17.9	4.3	9.6

[a] Observed in argon matrix.

The other resonances likely to be present involve ν_sCD$_3$, ν_sCH$_2$, ν_{as}CD$_2$, and ν_sCD$_2$ in the d$_6$, d$_2$, d$_4$, and d$_4$ species, respectively. The absence of bands associated with the overtone or combination levels concerned prevents further exploration of these. However, we note that ν_{as}CD$_2$ at 2222 cm^{-1} lies 3 cm^{-1} below ν_{as}CD$_3$ at 2225 cm^{-1}, a common feature that has previously been recognized as due to a resonance in the former with the combination δCH (A′) + δCH (A″), calculated here to lie near 2309 cm^{-1}.[25] In the HLM approximation, ν_{as}CD$_3$ and ν_{as}CD$_2$ are identical in frequency.

Looking at all the data together, we feel confident that the H−C−H angle lies between 108 and 110° and therefore quote 109 ± 1° as the best available estimate.

When the matrix data are examined in a similar way, there are great difficulties. As demonstrated in Table 19, ν_{as}CH$_3$ and ν_{as}CD$_3$ are incompatible over the range of angle 107−111° and become compatible only at the improbable angle of 99°. It is very unlikely, too, that the Fermi resonance correction for ν_sCD$_3$ is greater than that for ν_sCH$_3$. Part of the explanation for these unprecedented anomalies may lie in the pronounced overlap of Me$_2$TiCl$_2$ and methane bands, which bedevils many of the matrix spectra. In the meantime, no inference concerning the H−C−H angle in the matrix-isolated molecule can be drawn from these results.

General Discussion

Methyl Group Structure. The ν^{is}CH values of 2938 and 2952.3 cm^{-1} for Me$_2$TiCl$_2$ and MeTiCl$_3$, respectively, lead via the established correlation of ν^{is}CH with r_0CH,[14]

$$r_0(\text{Å}) = 1.3982 - 0.0001023\nu^{is}\text{CH (cm}^{-1})$$

to the prediction of r_0 bond lengths of 1.0976 and 1.0962 Å. The bond lengths concerned are based on spectroscopic inertial constants and are not therefore equilibrium values. However, each "equilibrium" value given by a QM calculation will also differ from the true one by some "offset" factor. Nevertheless, trends and differences of bond length indicated by the two kinds of study should be closely parallel. Thus, the lengthening in r_0 on passing from the mono- to the dimethyl compound, although small, is quite well reproduced by both DFT calculations, albeit less well by the MP2 one, where the change is negligible.

In principle, information about the H−C−H angle can be obtained in three ways.

(i) A limited correlation holds between ν^{is}CH and the H−C−H angle of a methyl group:[12,13]

$$\text{H−C−H (deg)} = 31.12 - 0.04709\nu^{is}\text{CH (cm}^{-1})$$

While this had not been thought earlier to apply to methylmetal compounds, recent quantum mechanical calculations involving

Me$_2$M compounds (M = Zn, Cd, or Hg)[26] suggest that the gradient of such a plot may be applicable, if not the intercept. A decrease of 0.7° in the H−C−H angle would then be anticipated on going from MeTiCl$_3$ to Me$_2$TiCl$_2$.

(ii) A second method is to use the observed ratio ν_{as}CH$_3$/ ν_{as}CD$_3$, which is mildly sensitive to the H−C−H angle. This approach has the disadvantage of requiring the rather accurate location of the band center for each of the two bands concerned; it also involves the assumption of a correction factor to allow for the effects of anharmonicity. In the case of MeTiCl$_3$[5] the ratio gave quite good agreement (within 0.7°) with the electron diffraction[4] and computed[3,16] values of the H−C−H angle. In the present case of Me$_2$TiCl$_2$, however, the two bands concerned are not sufficiently well defined, especially that due to ν_{as}CH$_3$, and accordingly no meaningful estimate of the H−C−H angle can be made in this way.

(iii) The third method depends on the overall fit in a harmonic local mode analysis, as discussed above. The angle of 109 ± 1° that this procedure yields for Me$_2$TiCl$_2$ (q.v.) means that we are predicting a decrease of about 1° in H−C−H from the best *ab initio* estimate in MeTiCl$_3$. Although the changes concerned here are small, it is interesting to note that a typical comparison of *ab initio* and ν^{is}CH predictions of bond length shows that, where there are large changes, as in Me$_3$N, the *ab initio* estimate of the difference is likely to be about two-thirds of the estimate afforded by ν^{is}CH.[20]

A possible discrepancy of a different kind is that between the H−C−H angle as deduced here from the C−H stretching frequencies and that determined by electron diffraction. The latter method yields in the first place the Ti−C−H angle, which in the r_a structure is found to be 102.6°.[9] For a symmetrical methyl group, this would imply that H−C−H = 115.4°, suggesting a substantial flattening of the unit. Once amplitude corrections derived from the unscaled DFT/AE force field are introduced, though, the estimated Ti−C−H angle increases to 108.1 ± 1°.[9] The fact that the amplitude correction is so large makes it possible that the method of estimating it is significantly in error, so that the 2° difference between the electron diffraction and IR-based values of the H−C−H angle is unimportant. Scaling of the force field used to supply the perpendicular amplitudes involved and a more realistic description of the torsional and free rotor states of the methyl groups could both be studied with profit.

Use of ν^{is}CD Data. ν^{is}CD data offered one of the earliest ways of identifying individual C−H bond strengths and have been taken up again more recently.[15] They have the obvious advantage of easier methods of preparation but suffer the disadvantages (i) of occurring at lower energies in the spectrum, with the result that a higher proportion of bending motion is present in the normal coordinate, and also (ii) of a greater propensity to overlap with overtone or combination bands with the possible ensuing interference from Fermi resonance. Such resonance is rare or insignificant in the νCH region of the spectrum when ν^{is}CH bands are recorded. It is important therefore to study as many systems as possible for which both ν^{is}CH and ν^{is}CD data are available, if there is to be confidence in the quantitative use of the latter. The results for Me$_2$TiCl$_2$ reported here suggest that, within the limits determined by not very precisely defined band centers, the two kinds of data are fully compatible, with due allowance for the usual anharmonicity correction factor of 1.011.[23]

While this result is encouraging, further systems need to be studied and a careful search has to be mounted for Fermi resonances before the more widespread use of this technique can be advocated.

1966 *J. Phys. Chem. A, Vol. 101, No. 10, 1997*

McGrady et al.

Force Constant Scaling Procedure. The scale factors in an SQM harmonic force field reflect, on one hand, the defects of the QM approach chosen and, on the other, the extent to which the experimental data used in the scaling are affected by anharmonicity, which, *inter alia*, introduces a degree of incompatibility between the data from different isotopomers. When steps are taken to correct even approximately the experimental data for anharmonicity, as in ref 20, there is a clear tendency for the scale factors to approach one another, and to approach unity, as the level of the QM treatment is raised. Anharmonicity corrections were not considered to be appropriate in the present study of MeTiCl$_3$, but their lack need not vitiate comparisons of the scale factors for assessing the merits of the various QM approaches involved (see Table 5). The corrections involved are unlikely to exceed about 1% except in the case of CH bending and stretching motions, where they are likely to be about 2% and 4%, respectively.[20,21]

The QM calculations reported presently (DFT/AE, DFT/ECP, MP2/ECP) generally employ basis sets of TZ2P quality (triple-ζ with two sets of polarization functions), except for DFT/AE, where the ligand atoms are described by a TZP basis. We have carried out additional QM calculations with smaller basis sets (ranging from DZP to TZP, not reported presently) and have applied the scaling procedure to the resulting force fields. As expected, improvement in the size of the basis set, *e.g.* among the various MP2 calculations, leads to scale factors closer to unity, with occasional exceptions (ρCH$_3$). However, there was no evidence with MeTiCl$_3$ that the most modest MP2 treatment (DZP basis) necessitated more scale factors than the most elaborate one (TZ2P basis) nor that the corresponding predictions for Me$_2$TiCl$_2$ after scaling were significantly worse. We conclude that, with thorough scaling, a modest basis of DZP quality may yet produce satisfactory results. More evident are differences between the scaled MP2 results on one hand and the scaled DFT results on the other. Regardless of the basis set employed, the latter results turn out to be superior in the case of MeTiCl$_3$ and Me$_2$TiCl$_2$.

Other interesting features are the variability and unpredictability of the scale factors involved. This alone constitutes an argument for scaling such force fields with closer attention than is commonly given at the present time, when the number of factors is kept to a minimum, possibly only one. Particularly worrying is the uncritical acceptance of the normal coordinates accompanying such minimal scaling exercises. In situations where several normal modes are composed of highly coupled motions, whose individual symmetry force constants should in the relevant QM approach differ somewhat one from another, the use of a single common scale factor is bound to result in a significant misrepresentation of the coupling. This in turn will result in a poor calculation of the corresponding spectral intensities.

If experimental results from only one isotopomer are used in the scaling, the situation may remain undetected. When data for several species are available, as in the present cases of MeTiCl$_3$ and Me$_2$TiCl$_2$, the need for several scale factors will become apparent. However, it may also be found, as here with MeTiCl$_3$, that such data cannot be fitted by any number of scale factors within a scaling scheme in which off-diagonal constants are tied to the diagonal ones, because some small off-diagonal constant is being calculated incorrectly by an amount that is small in absolute terms but large in percentage terms. MeTiCl$_3$ constitutes the fourth such case to have been identified, the others being CH$_3$CH$_2$Cl,[18] Si$_2$H$_5$Cl,[19] and ketene.[27] More such cases will undoubtedly emerge as more thorough studies are made.

Experimental Section

Synthesis and Spectroscopic Measurements. The reactivity and instability of Me$_2$TiCl$_2$ noted above required that all manipulations had to be carried out in a high-vacuum system ($<ca.$ 10^{-4} Torr) in apparatus constructed from Pyrex glass. The only other materials allowed to come into contact with the compound were Teflon-PTFE, halocarbon grease, and CsI. All apparatus was thoroughly conditioned by exposure to dimethylzinc vapor prior to use; alternatively and additionally, glass surfaces were flamed to remove the last traces of moisture, or other volatile contaminants.

Early experience showed that the preparation of Me$_2$TiCl$_2$ according to eq 1 was nonstoichiometric, presumably on account of the decreased methylating capacity of the intermediate methylzinc chloride. Accordingly, at least a 2-fold excess of Me$_2$Zn was used in every preparation. Two routes were employed.

$$\text{Me}_2\text{Zn} + \text{TiCl}_4 \rightarrow \text{Me}_2\text{TiCl}_2 + \text{ZnCl}_2 \qquad (1)$$
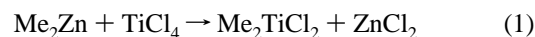
Samples for gas-phase analysis were synthesized *in situ* in a purpose-built IR cell. With a path length of 20 cm and a diameter of 21 mm, this consisted of a Pyrex glass body to which was attached a cold finger and a U-trap. The cold finger was isolated from the cell by a greaseless valve (J. Young, London). The U-trap was joined directly to the opposite side of the cell body and was closed at the far end, also by means of a Young's valve. Access to the vacuum line was through a ground-glass cone attached to this trap. In a typical preparation, Me$_2$Zn vapor was admitted to the cell to a pressure of 15−20 Torr. The cell was then isolated and the Me$_2$Zn condensed in the cold finger, which was also isolated. The cell was reopened to the vacuum line and TiCl$_4$ admitted to a pressure of 5−7 Torr. Once the cold finger had warmed to ambient temperature, the cell was again isolated from the vacuum line and the valve separating the cold finger from the cell body opened. Immediate reaction was observed to occur, with the concomitant deposition of a brown film on the internal surfaces of the vessel, and also in the vicinity of the valve. The excess of Me$_2$Zn was removed by opening the valve to the vacuum line and pumping the volatile material into the U-trap held at −63 °C, which retained the Me$_2$TiCl$_2$. At this stage the red-brown solid Me$_2$TiCl$_2$ was sublimed into the cold finger and isolated while the cell background was recorded. The vapor of the solid was then readmitted to the cell and its spectrum measured.

Samples for matrix-isolation studies were prepared in hydrocarbon solution. In a typical experiment, TiCl$_4$ (1.0 g; 5.3 mmol) and *n*-pentane (15 cm^3) were condensed in a reaction vessel equipped with a Young's valve and magnetic stirrer bar. Cocondensation of Me$_2$Zn (1.0 g; 10.6 mmol) at −196 °C, followed by cautious warming, led to immediate production of a dirty-brown precipitate and a purple-black solution that turned yellow on warming above *ca.* 50 °C. The mixture was then stirred at −20 °C for *ca.* 10 min to ensure complete reaction. The vessel was subsequently attached to a train of U-traps and the volatile material fractionated several times between traps held at −24, −63, and −196 °C. The middle fraction was shown to be pure on the basis of its ^{1}H NMR[8] and IR spectra. Samples were stored in break-seal ampules at −196 °C until required. Deposition of a yellow-brown involatile substance on the walls of the distillation train and of a deep brown solid at the point of condensation attested to the instability of the compound.

Despite the precautions taken, the spectra of both gaseous and matrix samples contained weak absorptions due to methane

(arising from decomposition in the cell) and to traces of Me₂-Zn derived from the preparation.

Starting materials were prepared as follows. Dimethylzinc was obtained from the reaction of iodomethane with a zinc/copper couple.[28] The partially deuterated species CH_2DI and CHD_2I were prepared from the corresponding chlorides,[29] which were themselves synthesized by the reaction of Bu^n_3SnD with CH_2BrCl or $CHBr_2Cl$, respectively.[30] CD_3I was derived from the reaction of CD_3OD with PI_3.[31]

IR spectra of gaseous samples were recorded in the region $4000-400$ cm^{-1} using a Mattson Galaxy FTIR spectrometer at a resolution of 1 cm^{-1}. Typically 100 scans were collected. Spectra of gaseous samples in the region $400-200$ cm^{-1} and of matrix-isolated samples in the region $4000-200$ cm^{-1} were measured using a Perkin-Elmer 580B dispersive spectrometer at an optimum resolution of 1.7 cm^{-1}. Raman spectra were measured for solutions in CCl_4 and C_6H_6 using a Perkin-Elmer 1700X FT-Raman spectrometer at a resolution of 4 cm^{-1}. Typically 50 scans were collected.

Thermal Decomposition Studies. The decomposition of Me₂TiCl₂ in solution has previously been examined by Mc-Cowan *et al.*,[32] who concluded that the reaction pathway was complex but that in dilute halocarbon solution the compound has a half-life of *ca.* 24 h. As is evident from Figures 1 and 2, Me₂TiCl₂ decomposes in all phases with the production of methane and a brown, involatile solid of indeterminate composition.[32] The present study yielded no IR spectrum in which bands arising from methane were absent. Inspection of Figures 1 and 2 and of Tables 8–11 reveals two features of note.

(i) There appears to be a substantial kinetic isotope effect to the decomposition; in both gas and matrix phases the amount of CH_4 present (3018, 1306 cm^{-1})[33,34] (Figures 1 and 2a,e) is substantially greater than that of CD_4 (2259, 996 cm^{-1})[33,34] (Figures 1 and 2d,g).

(ii) The presence of only CD_4 in the spectrum of $(CD_3)_2$-TiCl₂ indicates that the source of methane production is exclusively molecular decomposition and not, for example, reaction with residual moisture or other hydrogen-bearing foreign material in the apparatus.

In an attempt to characterize the decomposition more fully, a mixture of separate samples of $(CH_3)_2TiCl_2$ and $(CD_3)_2TiCl_2$ was admitted to the gas cell and the spectrum studied as a function of time. The presence of infrared bands due only to the h₄ and d₄ isotopomers of methane indicates (a) that decomposition in the gas phase occurs exclusively by an intramolecular pathway, and (b) that methyl group exchange does not occur to any measurable extent under the same conditions. The half-life of the sample under these conditions (1–2 Torr in the dark) is of the order of several hours; any assessment of, for example, the order of reaction is complicated by the likely involvement of heterogeneous processes (*e.g.* reaction at cell or window surfaces) in the decomposition.

In a related experiment, the vapor above a solid mixed sample of $(CH_3)_2TiCl_2$ and $(CD_3)_2TiCl_2$ was observed as a function of time. In this case decomposition appeared to occur much more quickly, the half-life of the sample being approximately 1 h. Furthermore, absorptions at 2945 and 2200, and 2993 and 2142 cm^{-1} attested to the presence of the mixed isotopomers CH_3D and CHD_3, respectively,[33,34] indicating involvement of an intermolecular pathway in the decomposition process. As Me₂-TiCl₂ exists in the solid presumably in the form of dimers,[35] this observation is perhaps not surprising.

Quantum Mechanical Calculations. The quantum chemical calculations were carried out at the level of second-order Møller−Plesset perturbation theory (MP2)[36] and gradient-corrected density functional theory[37] using the program system Gaussian92/DFT.[38] Gradient corrections for exchange and correlation were taken from the work of Becke[39] and Perdew,[40a] respectively (abbreviated as BP86). In both types of calculation, titanium was described by a quasi-relativistic effective core potential and the corresponding (8s7p5d)/[6s5p3d] basis set.[41] Carbon and hydrogen were represented by (10s6p)/[5s3p] and (5s)/[3s] triple-ζ basis sets,[42] respectively, augmented by two sets of polarization functions.[43] For chlorine, we used a triple-ζ (12s9p/[6s5p] basis[44] supplemented with two sets of polarization functions.[45] The chosen basis is of TZ2P quality (triple-ζ plus double polarization). Spherical d functions were employed throughout. The equilibrium geometries of MeTiCl₃ and Me₂-TiCl₂ were fully optimized in the appropriate point group symmetry (C_{3v}, C_{2v}) using analytic energy gradients. Second derivatives were computed by numerical differentiation of the analytic gradient.

All-electron DFT calculations were also carried out using the BPW91 density functional with the gradient correction of Becke[39] for exchange and of Perdew−Wang[40b] for correlation. These utilized the program system Gaussian94.[46] Standard 6-311G(d) bases were used for C (11s5p1d)/[4s3p1d] and H (5s)/[3s],[47] along with the chlorine basis set proposed by McLean and Chandler (13s10p1d)/[6s5p1d],[48] the polarization exponent being 0.75. The primitive Gaussian basis set for titanium suggested by Wachters[49] was slightly modified by inclusion of two diffuse p orbitals (exponents 0.156 and 0.0611) and one diffuse d orbital (exponent 0.0743), giving a (14s11p6d)/[10s8p3d] basis set. Optimization proceeded under the assumption of C_{3v} or C_{2v} symmetry, respectively. The molecular force field was calculated using analytical derivative methods.[50]

Scaling of the various force fields was carried out using the program ASYM40,[51] an update of ASYM20[51] that inputs Cartesian coordinates and force constants from a Gaussian program output file and scales each diagonal symmetry constant F_{ii} by a factor s_{ii} and each off-diagonal constant F_{ij} by the geometric mean of the constants s_{ii} and s_{jj}.[52] Each force field was therefore calculated at the appropriate equilibrium geometry in Table 1. ASYM20 itself was used for the harmonic local mode analysis of the observed C−H and C−D stretching fundamentals.

References and Notes

(1) Berry, A.; Dawoodi, Z.; Derome, A. E.; Dickinson, J. M.; Downs, A. J.; Green, J. C.; Green, M. L. H.; Hare, P. M.; Payne, M. P.; Rankin, D. W. H.; Robertson, H. E. *J. Chem. Soc., Chem. Commun.* **1986**, 520.

(2) Williamson, R. L.; Hall, M. B. *J. Am. Chem. Soc.* **1988**, *110*, 4428.

(3) Krömer, R.; Thiel, W. *Chem. Phys. Lett.* **1992**, *189*, 105.

(4) Briant, P.; Green, J.; Haaland, A.; Møllendal, H.; Rypdal, K.; Tremmel, J. *J. Am. Chem. Soc.* **1989**, *111*, 3434.

(5) McKean, D. C.; McQuillan, G. P.; Torto, I.; Bednall, N. C.; Downs, A. J.; Dickinson, J. M. *J. Mol. Struct.* **1991**, *247*, 73.

(6) Gray, A. P.; Callear, A. B.; Edgecombe, F. H. C. *Can. J. Chem.* **1963**, *41*, 1502.

(7) Gray, A. P. *Can. J. Chem.* **1963**, *41*, 1511.

(8) Hanlan, J. F.; McCowan, J. D. *Can. J. Chem.* **1972**, *50*, 747.

(9) McGrady, G. S.; Downs, A. J.; McKean, D. C.; Haaland, A.; Scherer, W.; Verne, H. P.; Volden, H. V. *Inorg. Chem.* **1996**, *35*, 4713.

(10) McGrady, G. S.; Downs, A. J.; Hamblin, J. M.; McKean, D. C. *Organometallics* **1995**, *14*, 3783.

(11) Robertson, A. H. J.; McQuillan, G. P.; McKean, D. C. *J. Chem. Soc., Dalton Trans.* **1995**, 3941.

(12) McKean, D. C. *Chem. Soc. Rev.* **1978**, 7, 399.

(13) McKean, D. C. *Croat. Chem. Acta* **1988**, *61*, 447.

(14) McKean, D. C. *J. Mol. Struct.* **1984**, *113*, 251.

(15) Compare the following: (a) Krueger, P. J.; Jan, J. *Can. J. Chem.* **1970**, *48*, 3229, 3236. (b) Bose, P. K.; Henderson, D. O.; Ewig, C. S.; Polavarapu, P. L. *J. Phys. Chem.* **1989**, *93*, 5070. (c) Grajcar, L.; Baron, M. H.; Becouarn, S.; Czernecki, S.; Valery, J. M.; Reiss, C. *Spectrochim. Acta* **1994**, *50A*, 1015. (d) Ohno, K.; Takagi, Y.; Matsuura, H. *J. Phys. Chem.* **1993**, *97*, 5530. (e) Ohno, K.; Yoshida, H.; Matsuura, H. *Spectrochim. Acta* **1996**, *52A*, 1377.

(16) (a) Jonas, V.; Frenking, G.; Reetz, M. T. *J. Comput. Chem.* **1992**, *13*, 919. (b) Berger, S.; Bock, W.; Frenking, G.; Jonas, V.; Müller, F. *J. Am. Chem. Soc.* **1995**, *117*, 3820.

(17) Jonas, V.; Böhme, C.; Frenking, G. *Inorg. Chem.* **1996**, *35*, 2097.

(18) McKean, D. C.; McQuillan, G. P.; Robertson, A. H. J.; Murphy, W. F.; Mastryukov, V. S.; Boggs, J. E. *J. Phys. Chem.* **1995**, *99*, 8994.

(19) McKean, D. C.; McPhail, A. L.; Edwards, H. G. M.; Lewis, I. R.; Murphy, W. F.; Mastryukov, V. S.; Boggs, J. E. *Spectrochim. Acta* **1995**, *51A*, 215.

(20) Murphy, W. F.; Zerbetto, F.; Duncan, J. L.; McKean, D. C. *J. Phys. Chem.* **1993**, *97*, 581.

(21) McKean, D. C.; McQuillan, G. P.; Murphy, W. F.; Zerbetto, F. *J. Phys. Chem.* **1990**, *94*, 4820.

(22) For convenience, refinement of the νCH factor was made to ν^{is}CH$_s$ = 2938 cm^{-1}, ignoring the lower QM values calculated for ν^{is}CH$_a$. s and a denote hydrogen atoms that are, respectively, in and out of the plane of symmetry.

(23) McKean, D. C. *Spectrochim. Acta* **1992**, *48A*, 1335.

(24) Duncan, J. L.; Law, M. M. *J. Mol. Spectrosc.* **1990**, *140*, 13.

(25) Robertson, A. H. J.; McQuillan, G. P.; McKean, D. C. *J. Chem. Soc., Dalton Trans.* **1995**, 3955.

(26) Kippels, C.; Thiel, W.; McKean, D. C.; Coats, A. M. *Spectrochim. Acta* **1992**, *48A*, 1067.

(27) East, A. L. L.; Allen, W. D.; Klippenstein, S. J. *J. Chem. Phys.* **1995**, *102*, 8506.

(28) Hota, N. K.; Willis, C. J. *J. Organomet. Chem.* **1967**, *9*, 169.

(29) Hughes, E. D.; Ingold, C. K.; Mackie, J. D. H. *J. Chem. Soc.* **1955**, 3177.

(30) Green, M. L. H.; Hughes, A. K.; Popham, N. A.; Stephens, A. H. H.; Wong, L.-L. *J. Chem. Soc., Dalton Trans.* **1992**, 3077.

(31) Douglass, I. B. *Int. J. Sulfur Chem.* **1973**, *8*, 441.

(32) McCowan, J. D.; Hanlan, J. F. *Can. J. Chem.* **1972**, *50*, 755.

(33) Wilmshurst, J. K.; Bernstein, H. J. *Can. J. Chem.* **1957**, *35*, 226.

(34) Jones, L. H.; McDowell, R. S. *J. Mol. Spectrosc.* **1959**, *3*, 632.

(35) Antipin, M. Yu.; Troyanov, S. I; Struchkov, Yu. T.; Bresler, L. S. *Metalloorg. Khim.* **1988**, *1,* 111.

(36) Møller, C.; Plesset, M. S. *Phys. Rev.* **1934**, *46*, 618.

(37) Parr, R. G.; Yang, W. *Density-Functional Theory of Atoms and Molecules*; Oxford University Press: New York, 1989.

(38) Frisch, M. J.; Trucks, G. W.; Schlegel, H. B.; Gill, P. M. W.; Johnson, B. G.; Wong, M. W.; Foresman, J. B.; Robb, M. A.; Head-Gordon, M.; Replogle, E. S.; Gomperts, R.; Andres, J. L.; Raghavachari, K.; Binkley, J. S.; Gonzalez, C.; Martin, R. L.; Fox, D. J.; Defrees, D. J.; Baker, J.; Stewart, J. J. P.; Pople, J. A. *GAUSSIAN92/DFT*, Revision F.4; Gaussian: Pittsburgh, PA, 1993.

(39) Becke, A. D. *Phys. Rev.* **1988**, *A38*, 3098.

(40) (a) Perdew, J. P. *Phys. Rev.* **1986**, *B33*, 8822; **1986**, *B34*, 7406 (E). (b) Perdew, J. P.; Wang, Y. *Phys. Rev.* **1992**, *B45*, 13244.

(41) Dolg, M.; Wedig, U.; Stoll, H.; Preuss, H. *J. Chem. Phys.* **1987**, *86*, 866.

(42) Dunning, T. H., Jr. *J. Chem. Phys.* **1971**, *55*, 716.

(43) Dunning, T. H., Jr. *J. Chem. Phys.* **1989**, *90*, 1007.

(44) Huzinaga, S.; Andzelm, J.; Klobukowski, M.; Radzio, E.; Sakai, Y.; Tatewaki, H. *Gaussian Basis Sets for Molecular Calculations*; Elsevier: Amsterdam, 1984.

(45) Poirier, R.; Kari, R.; Csizmadia, I. G. *Handbook of Gaussian Basis Sets*; Elsevier: Amsterdam, 1985; Table 17.17.1.

(46) Frisch, M. J.; Trucks, G. W.; Schlegel, H. B.; Gill, P. M. W.; Johnson, B. G.; Robb, M. A.; Cheeseman, J. R.; Keith, T. A.; Petersson, G. A.; Montgomery, J. A.; Raghavachari, K.; Al-Laham, M. A.; Zakrzewski, V. G.; Ortiz, J. V.; Foresman, J. B.; Cioslowski, J.; Stefanov, B. B.; Nanayakkara, A.; Challacombe, M.; Peng, C. Y.; Ayala, P. Y.; Chen, W.; Wong, M. W.; Andres, J. L.; Repogle, E. S.; Gomperts, R.; Martin, R. L.; Fox, J. D.; Binkley, J. S.; Defrees, D. J.; Baker, J.; Stewart, J. J. P.; Head-Gordon, M.; Gonzales, C.; Pople, J. A. *Gaussian* 94; Gaussian, Inc.: Pittsburgh, PA, 1995.

(47) Krishnan, R.; Binkley, J. S.; Seeger, R.; Pople, J. A. *J. Chem. Phys.* **1980**, *72*, 650.

(48) McLean, A. D.; Chandler, G. S. *J. Chem. Phys.* **1980**, *72*, 5639.

(49) Wachters, A. J. H. *J. Chem. Phys.* **1970**, *52*, 1033.

(50) (a) Johnson, B. G.; Frisch, M. J. *Chem. Phys. Lett.* **1993**, *216*, 133. (b) Johnson, B. G.; Frisch, M. J. *J. Chem. Phys.* **1994**, *100*, 7429.

(51) Hedberg, L.; Mills, I. M. *J. Mol. Spectrosc.* **1993**, *160*, 117.

(52) Pulay, P.; Fogarasi, G.; Pongor, G.; Boggs, J. E.; Vargha, A. *J. Am. Chem. Soc.* **1983**, *105*, 7037.